The Primordial Cosmic banana from WMAP to Planck. *Warm (keV)Dark Matter from primordial fluctuations and observations*

Norma G. SANCHEZ
LERMA Observatoire de Paris & CNRS

15th Paris Cosmology Colloquium Chalonge 2011

CONTENTS

H de Vega, C Destri, NG. Sanchez :

« MCMC analysis of WMAP3 and SDSS data points to broken symmetry inflaton potentials and provides a lower bound on the tensor to scalar ratio", **Phys. Rev. D77, 043509 (2008)**

« Higher order terms in the inflaton potential and the lower bound on the tensor to scalar ratio r"**Annals Phys 326, 578 (2011)**

D. Boyanovsky, C. Destri, H. de Vega, N.G.Sanchez
"The Effective Theory of Inflation in the Standard Model of the Universe and the CMB+LSS data analysis "
Int. J. Mod. Phys. A. 24, 3669-3864 (2009)

C. Burigana, C. Destri, H. de Vega, A. Gruppuso, N. Mandolesi, P. Natoli, N.G. Sanchez « Forecast for the *Planck* precision on the tensor to scalar ratio and other cosmological parameters"

APJ 724 , 588-607 (2010)

# Standard Cosmological Model: ΛCDM $\Rightarrow$ ΛWDM

Dark Matter + Λ + Baryons + Radiation
begins by the Inflationary Era. Explains the Observations:

- Seven years WMAP data and further CMB data

- Light Elements Abundances

- Large Scale Structures (LSS) Observations. BAO.

- Acceleration of the Universe expansion:
  Supernova Luminosity/Distance and Radio Galaxies.

- Gravitational Lensing Observations

- Lyman α Forest Observations

- Hubble Constant and Age of the Universe
  Measurements

- Properties of Clusters of Galaxies

- Galaxy structure explained by WDM

Standard Cosmological Model: DM + Λ + Baryons + Rad

- Begins by the inflationary era. Slow-Roll inflation explains horizon and flatness.

- Gravity is described by Einstein's General Relativity.

- Particle Physics described by the Standard Model of Particle Physics: $SU(3) \otimes SU(2) \otimes U(1) =$ qcd+electroweak model.

- Dark matter is non-relativistic during the matter dominated era where structure formation happens. DM is outside the SM of particle physics.

- Dark energy described by the cosmological constant Λ.

The Universe is made of radiation, matter and dark energy

Plot showing $\frac{\rho_\Lambda}{\rho}$ vs. $\log(1+z)$, $\frac{\rho_{Mat}}{\rho}$ vs. $\log(1+z)$, and $\frac{\rho_{rad}}{\rho}$ vs. $\log(1+z)$
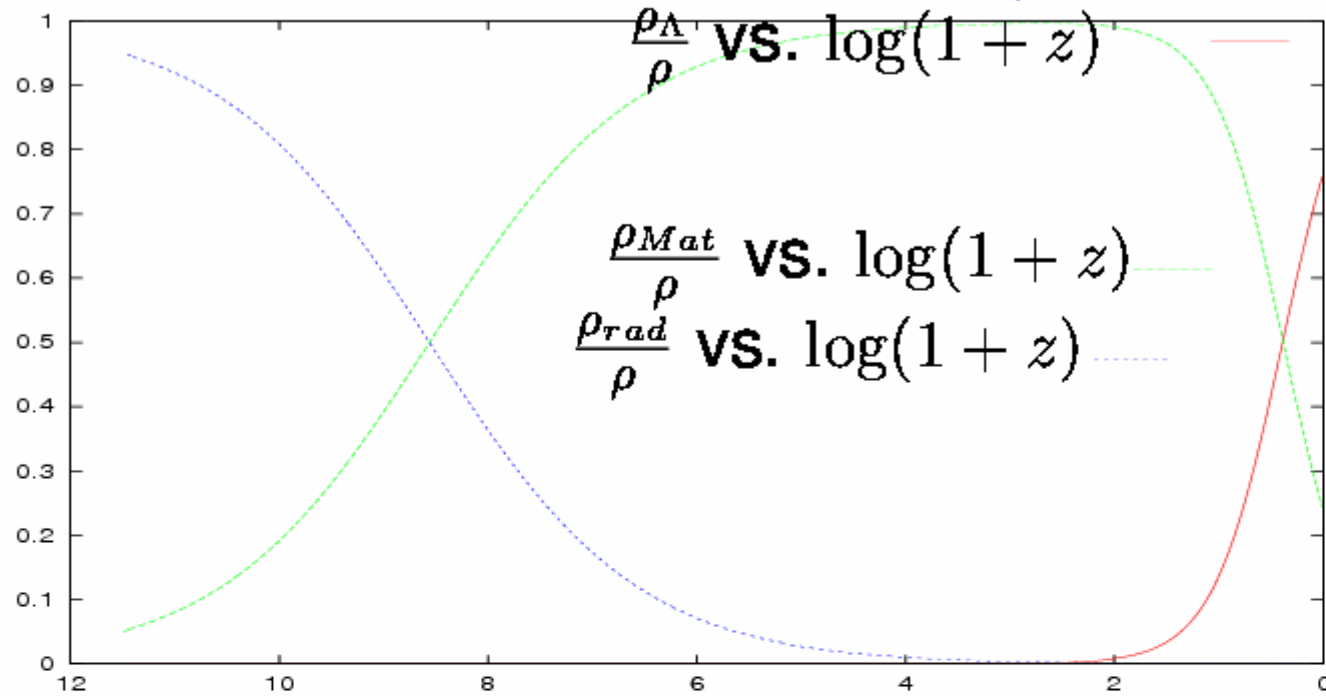
End of inflation: $z \sim 10^{29}$, $T_{reh} \lesssim 10^{16}$ GeV, $t \sim 10^{-36}$ sec.

E-W phase transition: $z \sim 10^{15}$, $T_{EW} \sim 100$ GeV, $t \sim 10^{-11}$ s.

QCD conf. transition: $z \sim 10^{12}$, $T_{QCD} \sim 170$ MeV, $t \sim 10^{-5}$ s.

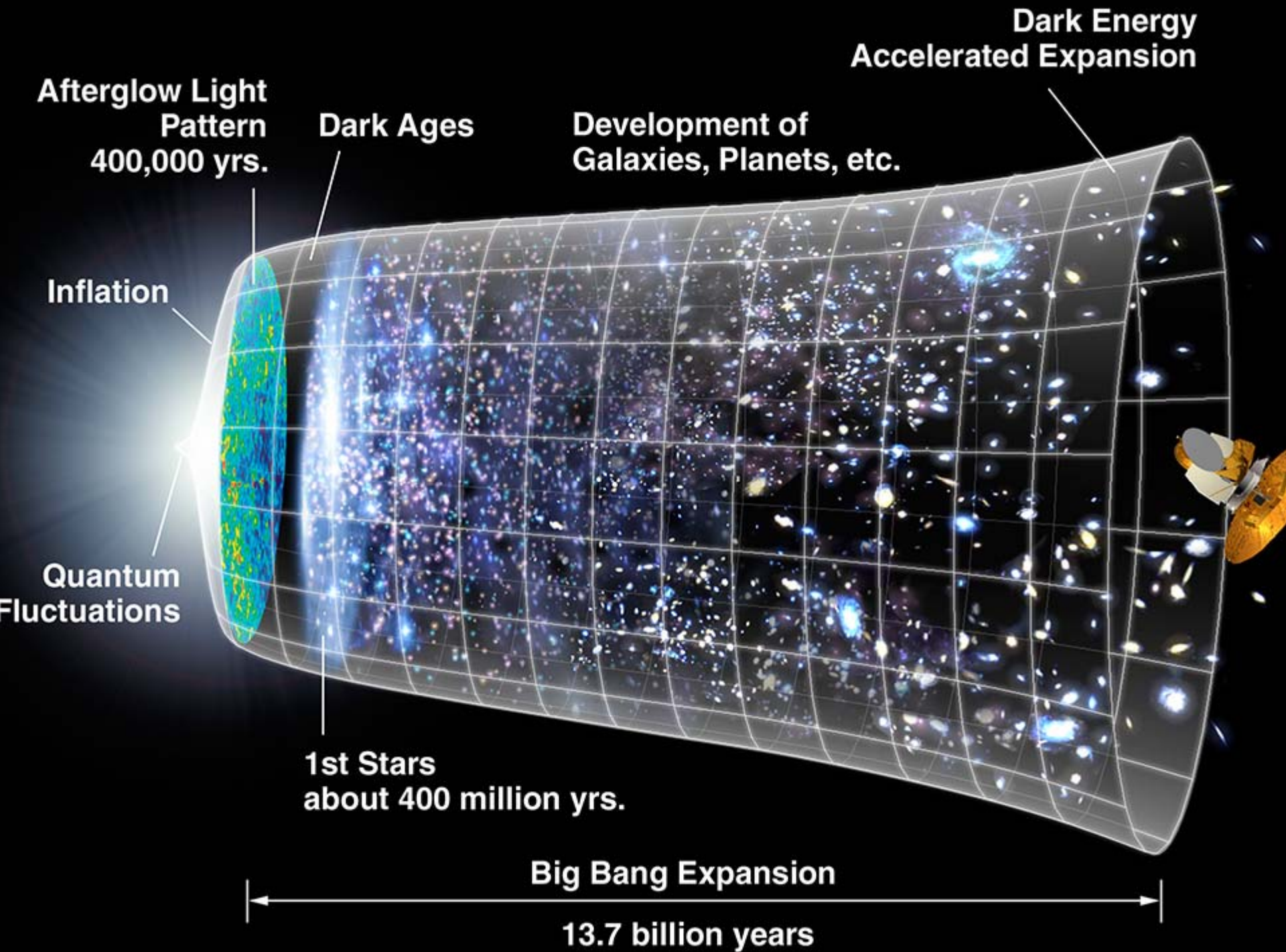BBN: $z \sim 10^{9}$, $T \simeq 0.1$ MeV, $t \sim 20$ sec.

Rad-Mat equality: $z \simeq 3200$, $T \simeq 0.7$ eV, $t \sim 57000$ yr.

CMB last scattering: $z \simeq 1100$, $T \simeq 0.25$ eV, $t \sim 370000$ yr.

Mat-DE equality: $z \simeq 0.47$, $T \simeq 0.345$ meV, $t \sim 8.9$ Gyr.

Today: $z = 0$, $T = 2.725$K $= 0.2348$ meV $t = 13.72$ Gyr.

Afterglow Light
Pattern
400,000 yrs.

Dark Ages

Development of
Galaxies, Planets, etc.

Dark Energy
Accelerated Expansion

Inflation

Quantum
Fluctuations

1st Stars
about 400 million yrs.

Big Bang Expansion

13.7 billion years

Quantum Fluctuations During Inflation and after

The Universe is homogeneous and isotropic after inflation thanks to the fast and gigantic expansion stretching lenghts by a factor $e^{62} \simeq 10^{27}$. By the end of inflation: $T \sim 10^{14}$ GeV.

Quantum fluctuations around the classical inflaton and FRW geometry were of course present.

These inflationary quantum fluctuations are the seeds of the structure formation and of the CMB anisotropies today: galaxies, clusters, stars, planets, ...

That is, our present universe was built out of inflationary quantum fluctuations. CMB anisotropies spectrum:

3×10^{-32}cm $< \lambda_{begin\,inflation} < 3 \times 10^{-28}$cm

$M_{Planck} \gtrsim 10^{18}$ GeV $> \lambda_{begin\,inflation}^{-1} > 10^{14}$ GeV.

total redshift since inflation begins till today $= 10^{56}$:

0.1 Mpc $< \lambda_{today} <$ 1 Gpc ,   1 pc $= 3 \times 10^{18}$ cm $= 200000$ AU
Universe expansion classicalizes the physics: decoherence

The Theory of Inflation

Inflation can be formulated as an effective field theory in the Ginsburg-Landau sense. Main predictions:

- The inflation energy scale turns to be the grand unification energy scale: $= 0.70 \times 10^{16}$ GeV

- The MCMC analysis of the WMAP+LSS data combined with the effective theory of inflation yields: a) the inflaton potential is a double–well, b) the ratio r of tensor to scalar fluctuations. has the lower bound:
  $r > 0.023 \ (95\% \ \mathrm{CL})$, $r > 0.046 \ (68\% \ \mathrm{CL})$ with $r \simeq 0.051$ as the most probable value.

This is borderline for the Planck satellite ($\sim 12/2012$?)
Burigana et. al. arXiv:1003.6108, ApJ to appear.
D. Boyanovsky, C. Destri, H. J. de Vega, N. G. Sánchez, (review article), arXiv:0901.0549, Int.J.Mod.Phys.**A 24**, 3669-3864 (2009).

LOWER BOUND on r
THE PRIMORDIAL GRAVITONS

Our theory input (Effective Theory Inflation) in the MCMC data analysis of WMAP5+LSS+SN data).

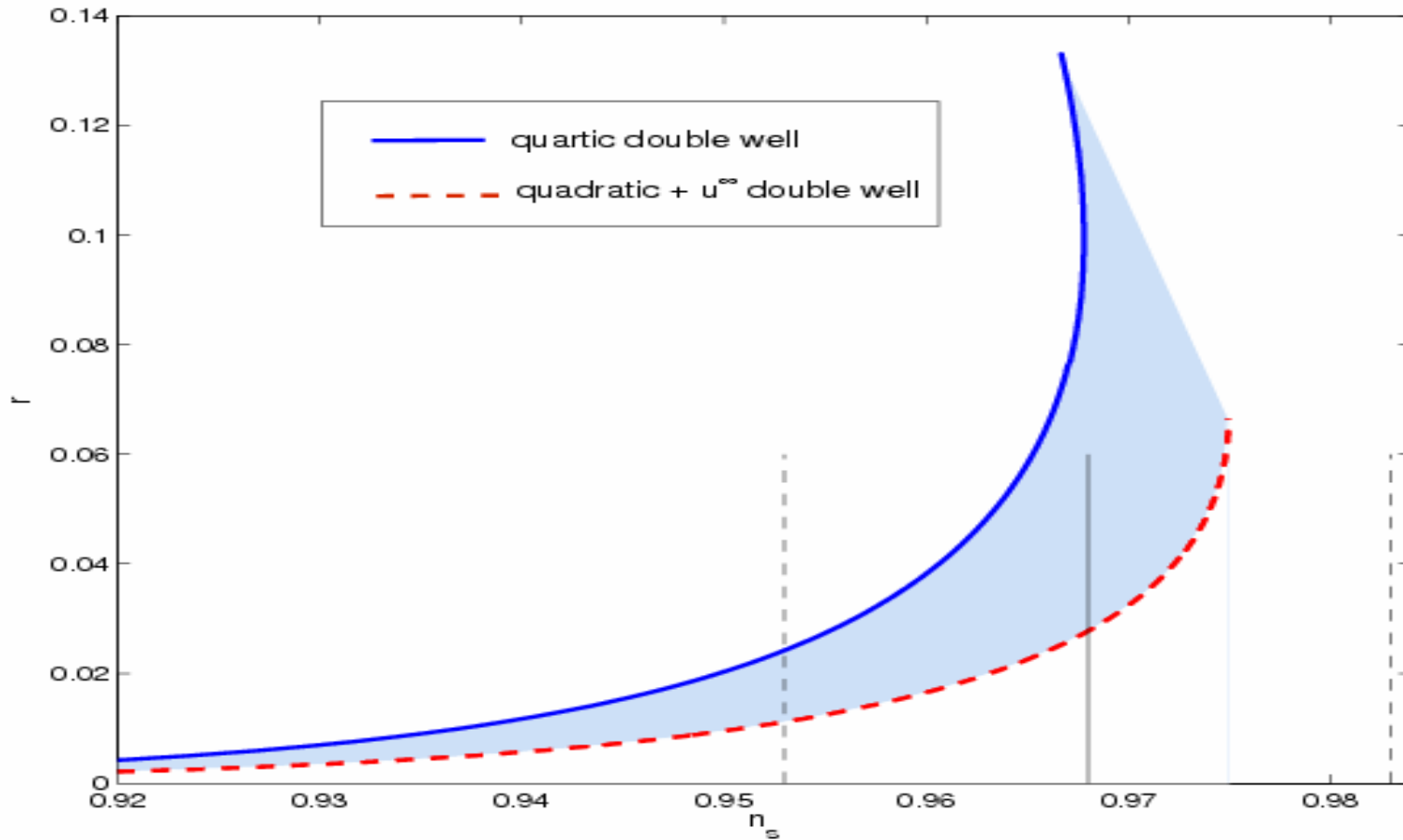**C. Destri, H J de Vega, N G Sanchez, Phys Rev D77, 043509 (2008) shows:**

Besides the upper bound for r (tensor to scalar ratio) $r < 0.22$, we find a clear peak in the r distribution and we obtain a lower bound

$$r > 0.023 \ \text{ at } \ 95\% \ \text{CL} \ \text{ and}$$

$$r > 0.046 \ \text{ at } \ 68\% \ \text{CL.}$$
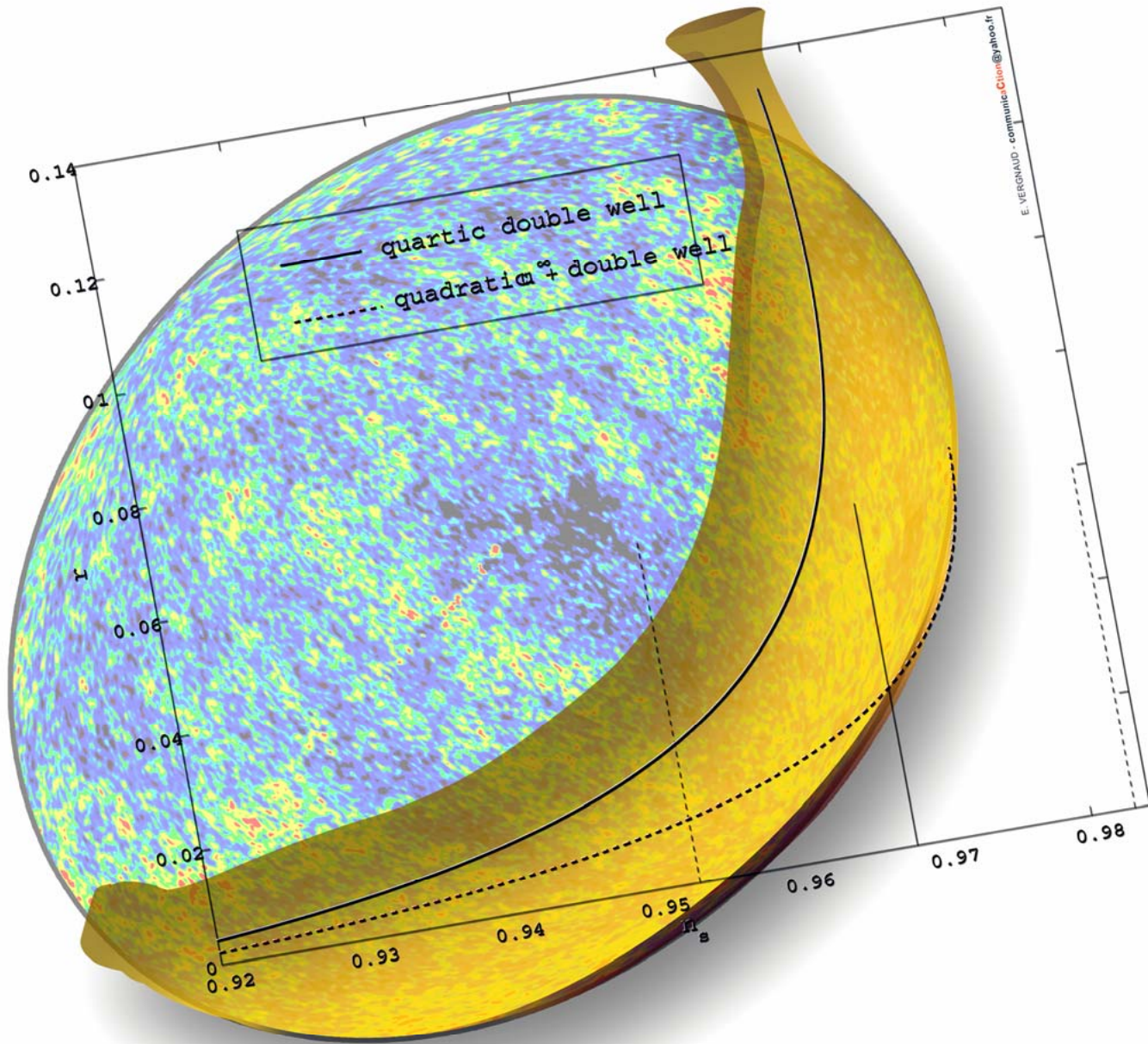
Moreover, we find $r = 0.051$ the most probable value

For the other cosmological parameters, both analysis agree.
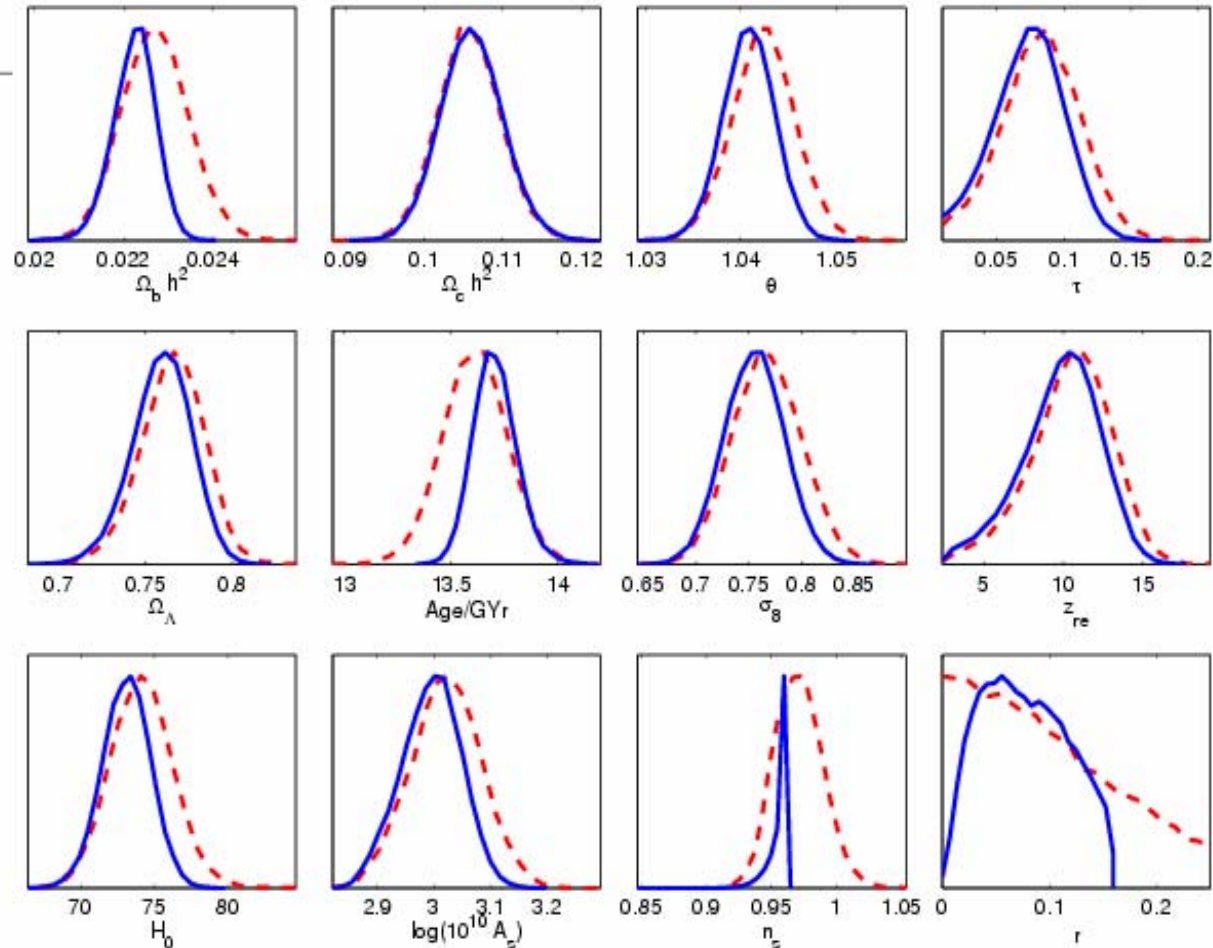
THE PRIMORDIAL COSMIC BANANA

The tensor to scalar ratio r (primordial gravitons) versus the scalar spectral index n_s. The amount of r is always non zero
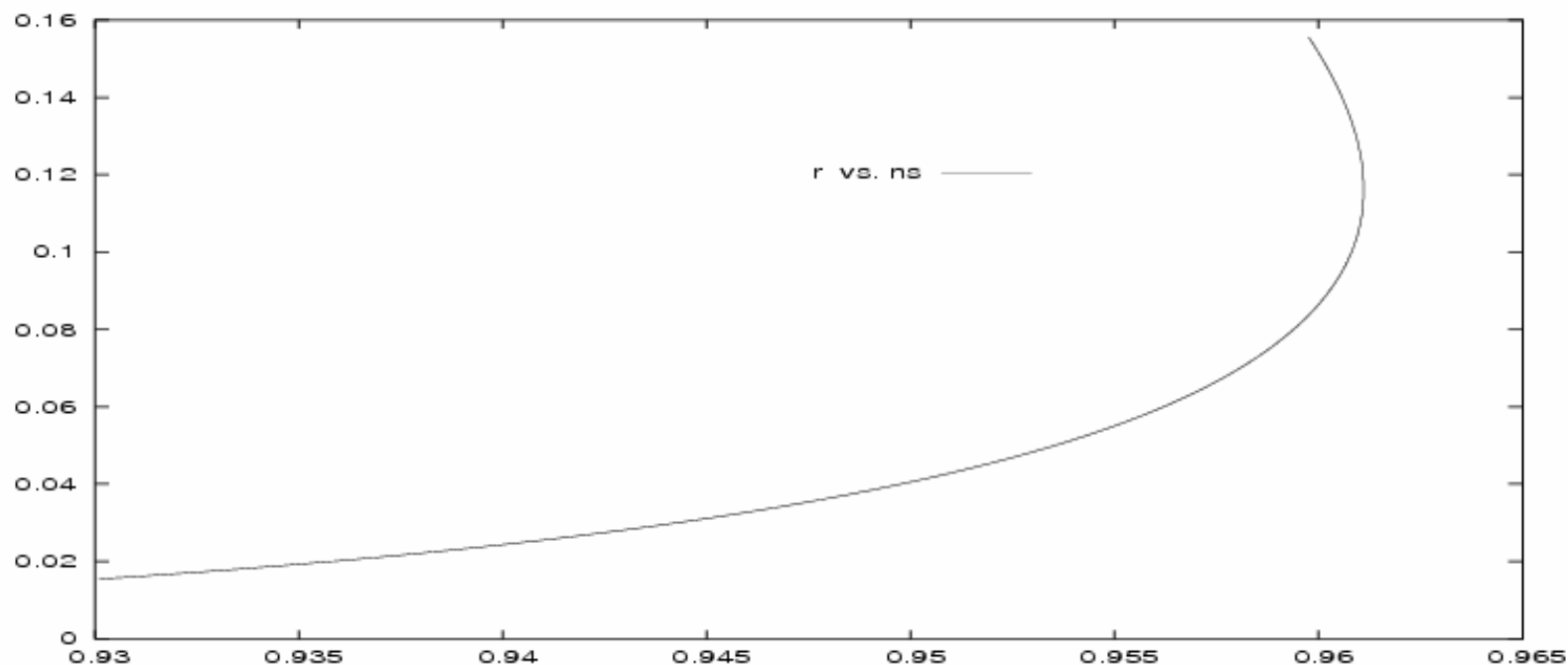
Marginalized probability distributions. New Inflation.

Imposing the trinomial potential (solid blue curves) and just the ΛCDM+r model (dashed red curves).
(curves normalized to have the maxima equal to one).
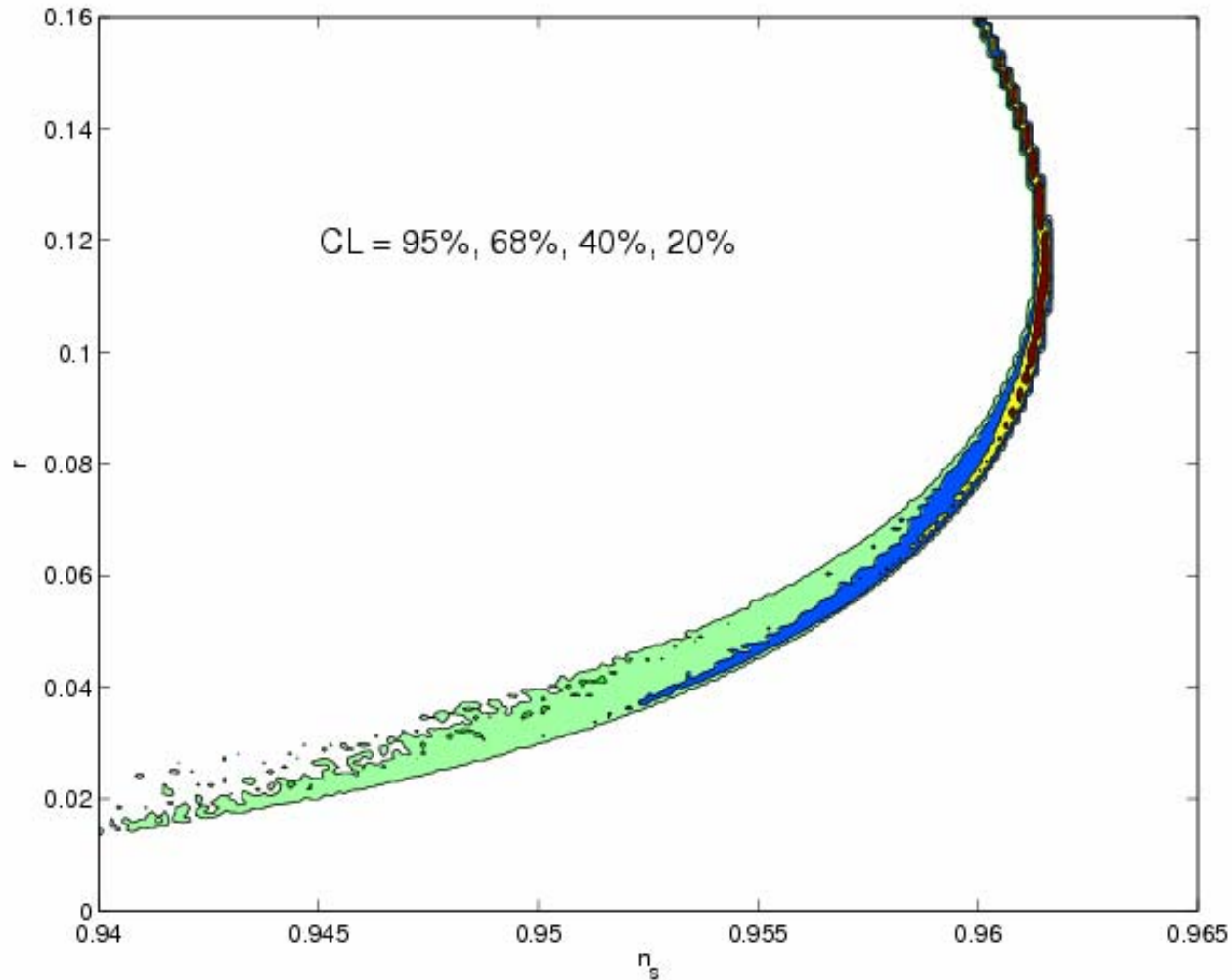
Binomial New Inflation

$r = \frac{8}{N} = 0.16$ and $n_s = 1 - \frac{2}{N} = 0.96$ at $y = 0$.

r is a double valued function of n_s.

r vs. n_s data within the Trinomial New Inflation Region.

CL = 95%, 68%, 40%, 20%

The sextic double–well inflaton potential
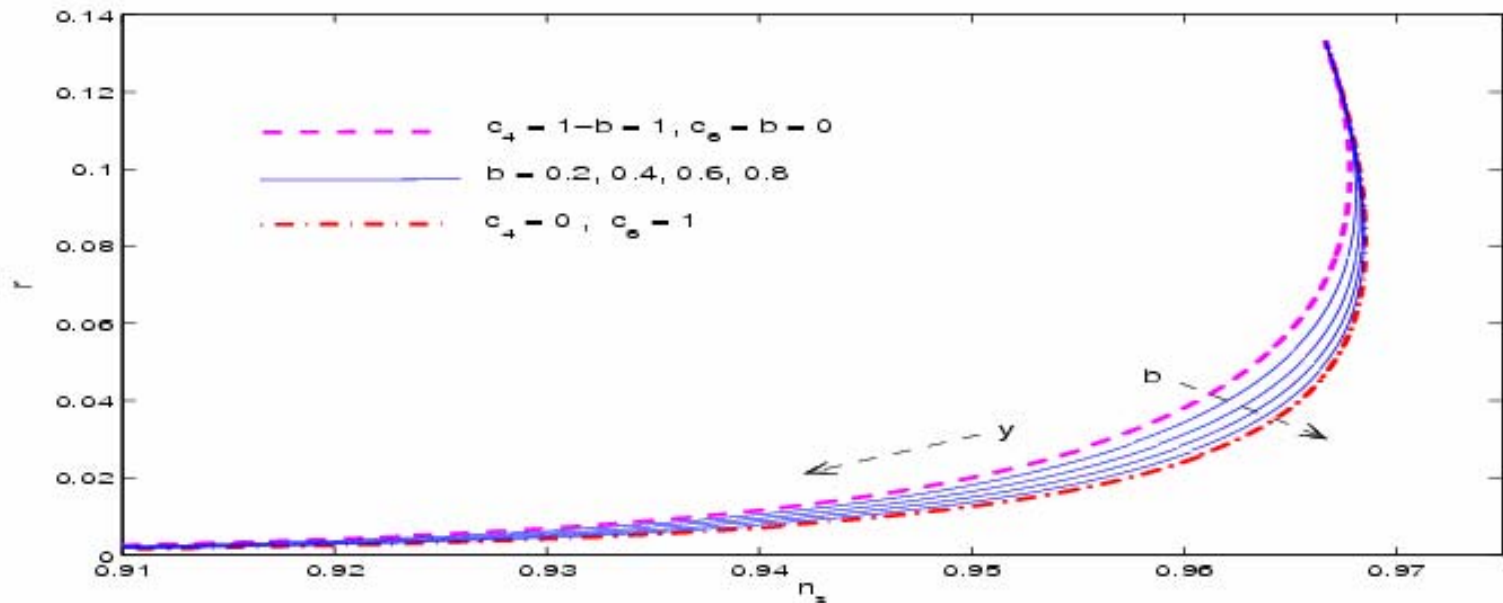
$$w_b(\chi) = \frac{y}{96} \left(\chi^2 - \frac{8}{y}\right)^2 \left(3 + b + \frac{1}{4} y \, b \, \chi^2\right) \; .$$

$0 < y < \infty$ coupling. $0 < b < 1$ shape-parameter.

$$w_{b=0}(\chi) = \frac{y}{32} \left(\chi^2 - \frac{8}{y}\right)^2 \quad \text{fourth order double–well.}$$

$$w_{b=1}(\chi) = \frac{8}{3y} - \frac{1}{2} \chi^2 + \frac{y^2}{384} \chi^6 \quad \text{sixth order double–well.}$$

The 100th degree polynomial inflaton potential
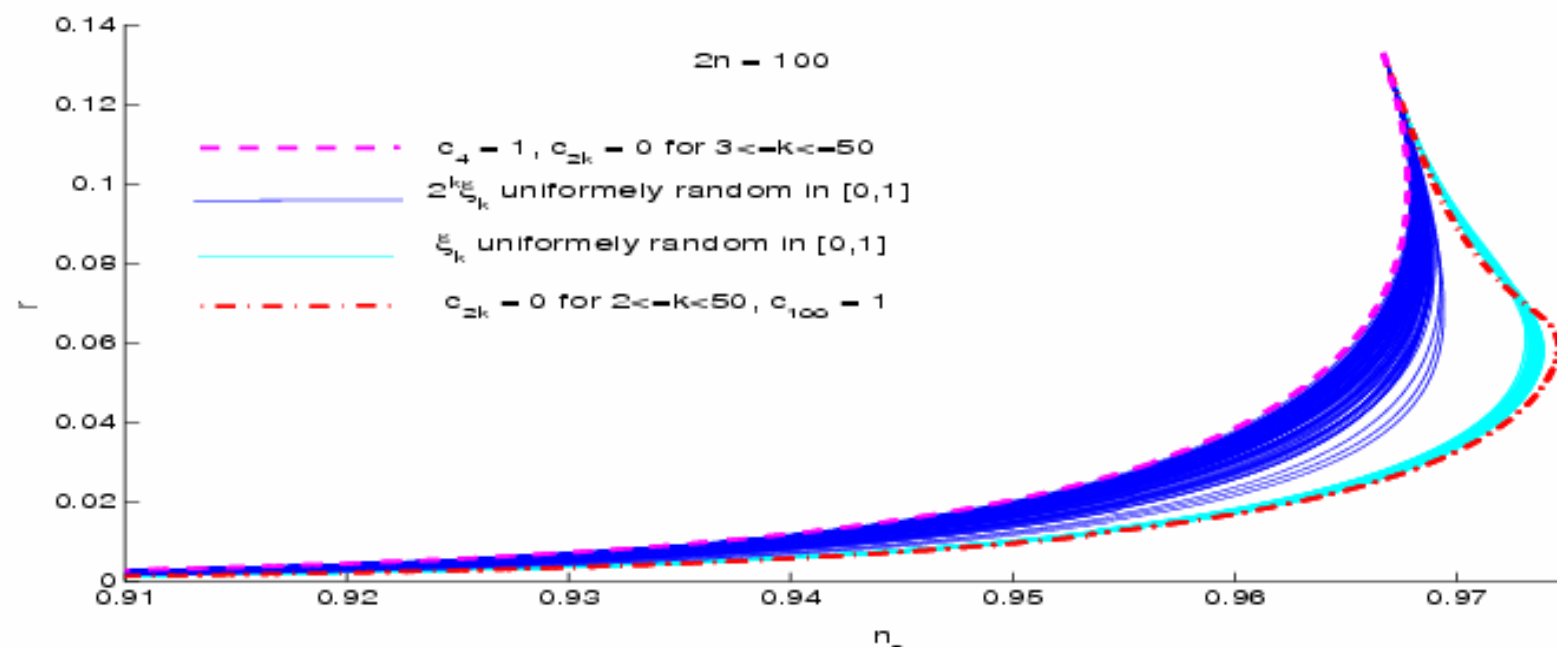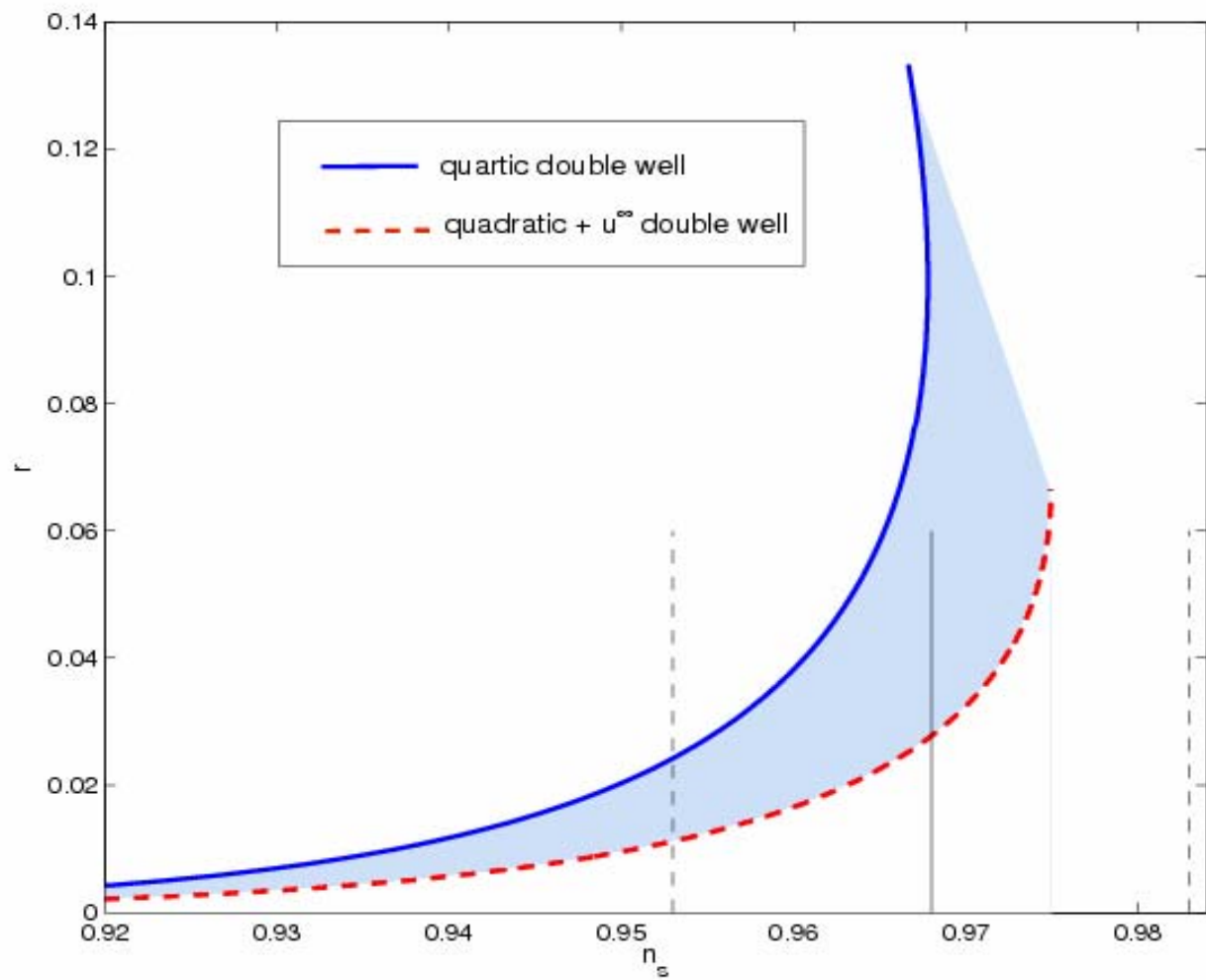

$$w(\chi) = \frac{4}{y} - \frac{1}{2}\chi^2 + \frac{4}{y}\sum_{k=2}^{n}\frac{c_{2k}}{k}\left(\frac{y^k}{8^k}\,u^{2k} - 1\right)$$

The coefficients c_{2k} were extracted at random.
The lower border of the banana-shaped region is given by the potential:

$$w(\chi) = \frac{4}{y} - \frac{1}{2}\chi^2 + \frac{4}{n\,y}\left(\frac{y^n}{8^n}\,u^{2n} - 1\right) \text{ with } n = 50.$$

PREDICTIONS From the cosmic banana:

UPPER BOUND $r < 0.053$

LOWER BOUND $r > 0.021$

$$0.021 < r < 0.053$$

Most probable value: $r \sim 0.051$

FORECASTS FOR PLANCK

With Fiducial $r = 0.0427$ • We found for r at 95% CL:

$0.028 < r < 0.116$

with the best values $r = 0.04$, $n_S = 0.9608$

C. Burigana, C. Destri, H.J. de Vega, A.Gruppuso, N. Mandolesi, P. Natoli, N. G. Sanchez :
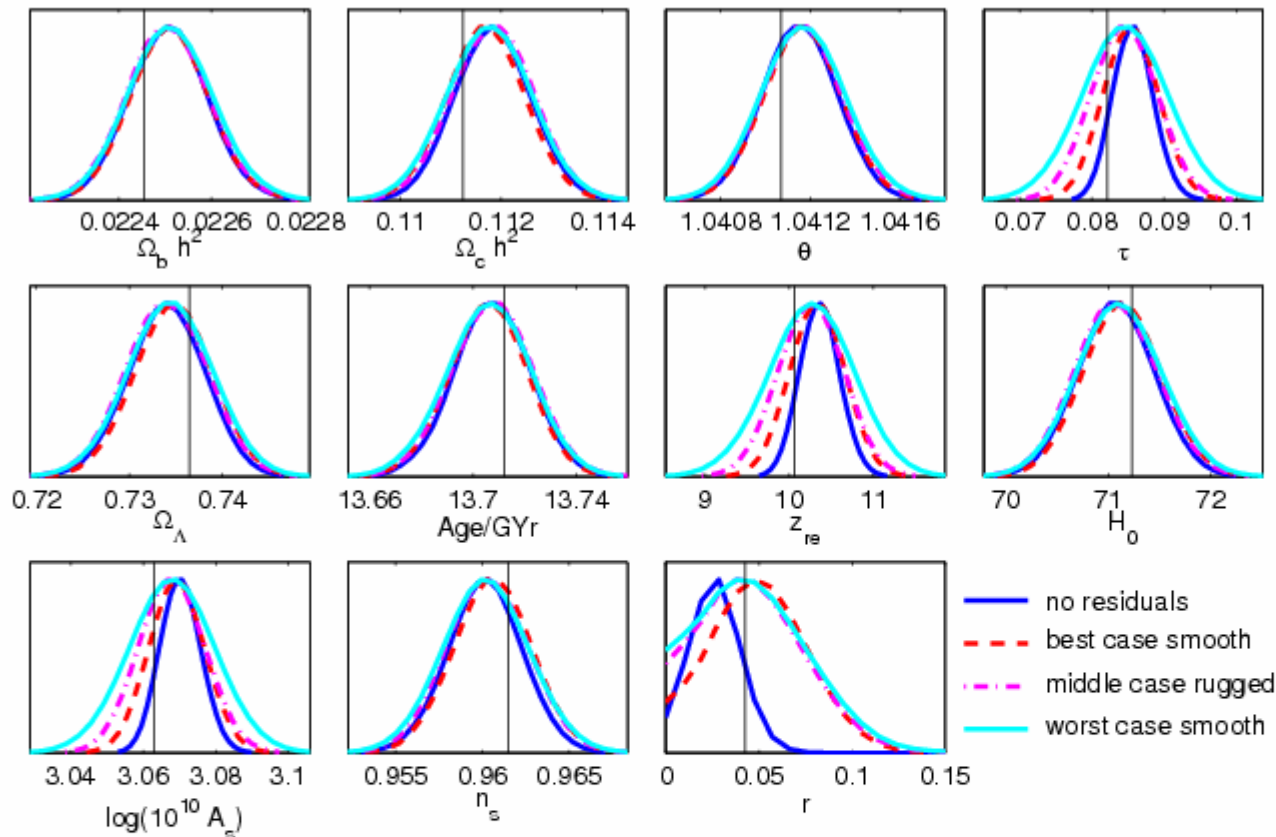
FIG. 7.— Cumulative 3—channel marginalized likelihood distributions, including B modes and foregroun[...] parameters for the $\Lambda CDMr$ model. The fiducial ratio is $r = 0$ in the upper panel and $r = 0.0427$ in the low[...] four cases: (a) without residuals, (b) with 30% of the toy model residuals in the TE and E modes displaye[...] modes, (c) with the toy model residuals in the TE and E modes displayed in Fig. 2 and $160\mu K^2$ in the T[...] model residuals in the TE and E modes displayed in Fig. 2 and $88\mu K^2$ in the T modes rugged by Gauss[...] strength.

FIG. 8.— Cumulative marginalized likelihoods from the three channels for the cosmological parameters for the ΛCDMrT model including *B* modes and fiducial ratio *r* = 0.0427 and the foreground residuals. We plot the cumulative likelihoods in four cases: (a) without residuals, (b) with 0.3 of the worst case residuals in the *TE* and *E* modes and $16\mu K^2$ in the *T* modes, (c) with the worst case residuals in the *TE* and *E* modes and $160\mu K^2$ in the *T* modes, (d) with 65% of the toy model residuals in the *TE* and *E* modes displayed in Fig. 2 and $88\mu K^2$ in the *T* modes rugged by Gaussian fluctuations of 30% relative strength.
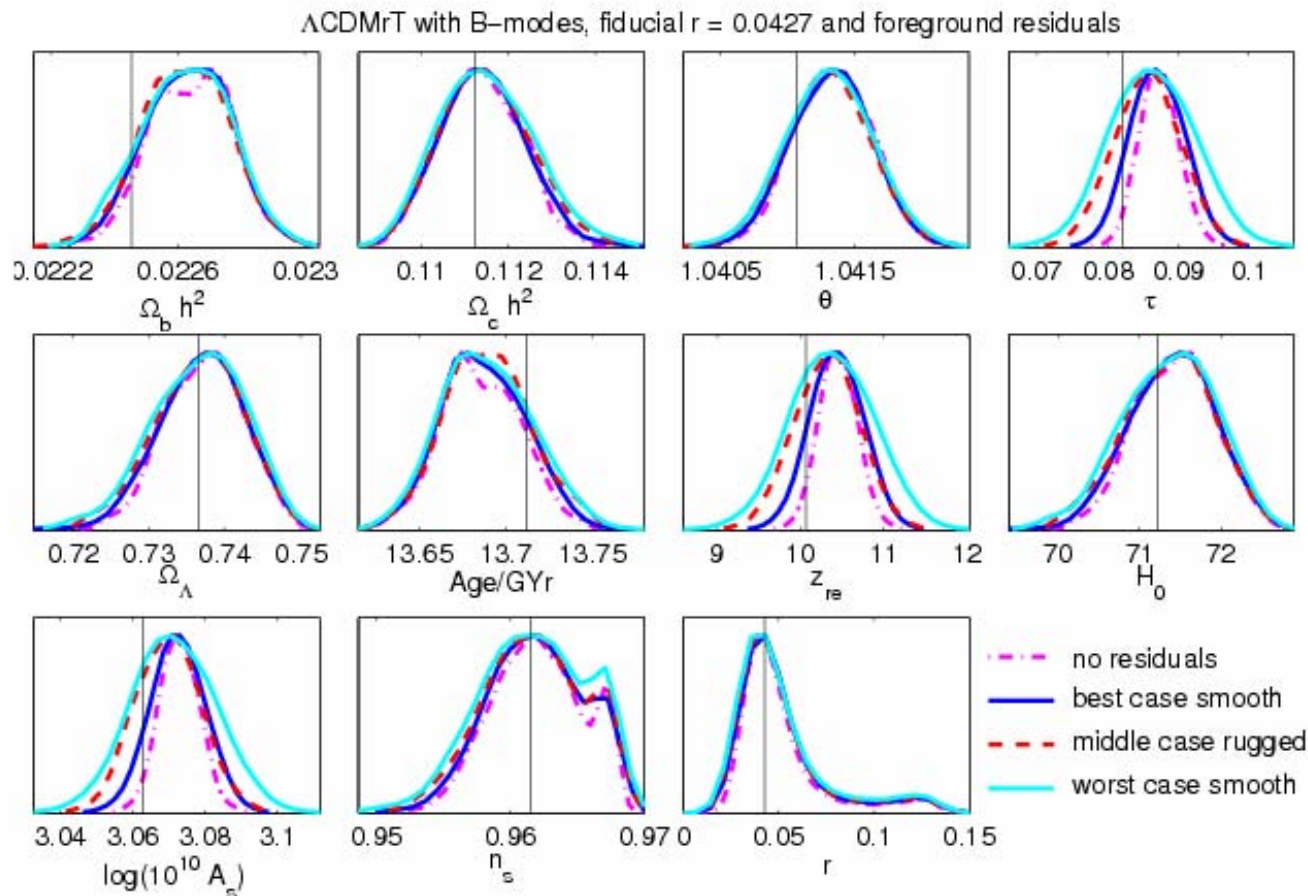
OUR FORECAST for PLANCK

$$0.028 < r < 0.116 \quad 95\% \quad CL,$$

best value $r = 0.04$ $\qquad n_s = 0.9608$

Supports searching of CMB B-mode polarization in the current data as well as the planned CMB polarization missions

→**Forecasted B mode detection probability by the most sensitive HFI-143 channel:**

→**For a 95% CL detection the level of foreground residual should be reduced to 10% or lower of the adopted toy model.** →**Borderline**

Dark Matter: from primordial fluctuations to Galaxies

❖ **Cold** (CDM): small velocity dispersion: small structures form first, **bottom-up** hierarchical growth formation, *too heavy (GeV)*

❖**Hot** (HDM) : large velocity dispersion: big structures form first, **top-down**, fragmentation, ruled out , *too light* (eV)

Warm (WDM): ``in between'' (keV)

ΛWDM Concordance Model:

CMB + LSS + SSS Observations
DM is WARM and COLLISIONLESS

CDM Problems:
- ➤ ⎰ clumpy halo problem'', large number of satellite galaxies
- ⎱ "satellite problem"
- ➤ ρ (r) ~ 1 / r (cusp)
- ➤ And other problems…..

Velocity widths in galaxies
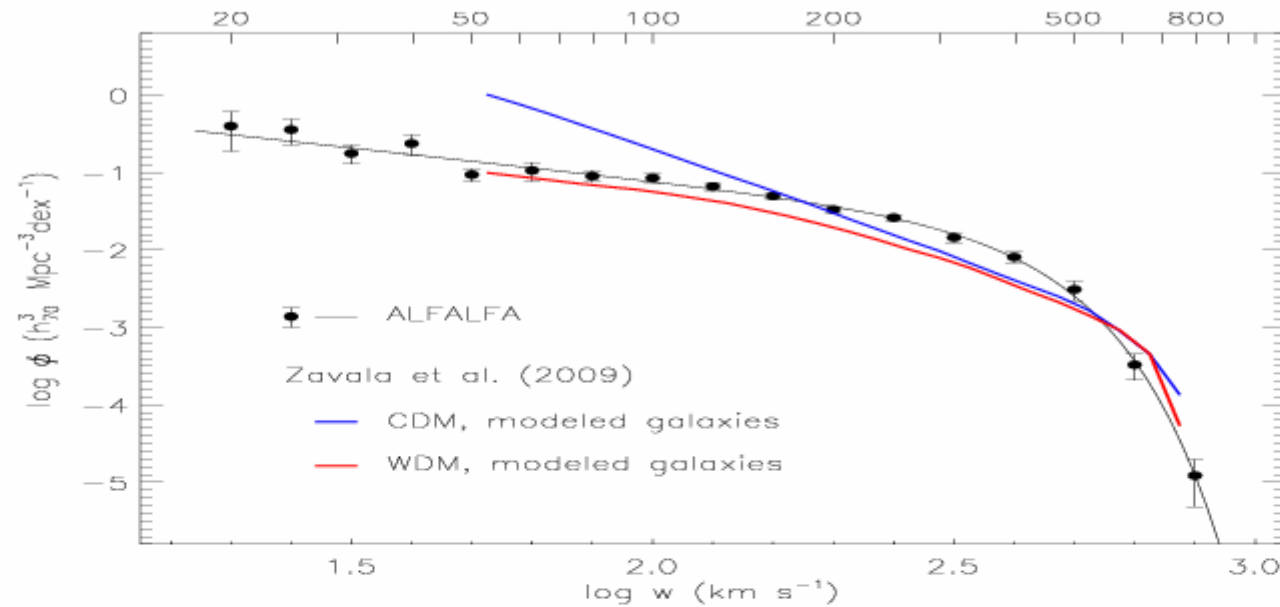
Velocity widths in galaxies from 21cm HI surveys. ALFALFA survey clearly favours WDM over CDM. (Papastergis et al. 2011, Zavala et al. 2009).

Notice that the WDM curve is for $m = 1$ keV.

THE MASS OF THE

DARK MATTER PARTICLE

MASS OF THE DARK MATTER PARTICLE

H. J. De Vega, N.G. Sanchez *Model independent analysis of dark matter points to a particle mass at the keV scale* Mon. Not. R. Astron. Soc. 404, 885 (2010)

D. Boyanovsky, H. J. de Vega, N.G. Sanchez *Constraints on dark matter particles from theory, galaxy observations and N-body simulations* Phys.Rev. D77 043518, (2008)

BOLTZMAN VLASOV EQUATION, TRANSFERT FUNCTION

D. Boyanovsky, H. J. de Vega, N.G. Sanchez *The dark matter transfer function: free streaming, particle statistics and memory of gravitational clustering* Phys. Rev. D78: 063546, (2008)

DENSITY PROFILES, SURFACE DENSITY, DARK MATTER PARTICLE MASS

H. J. de Vega, N.G. Sanchez *Gravity surface density and density profile of dark matter galaxies* IJMPA26:1057 (2011)

H. J. de Vega, P. Salucci, N.G. Sanchez *Universal galaxy properties and the mass of the dark matter particle from theory and observations: the power of the linear approximation* arXiv:1004.1908

→**Compute** from the distribution function of dark matter particles with their different statistics, physical magnitudes as :

-the dark matter energy density $\rho_{DM}(z)$,

-the dark matter velocity dispersion $\sigma_{DM}(z)$,

-the dark matter density in the phase space $D(z)$

→ **Confront** to their **values observed today** (z = 0).

→→ From them, the **mass m** of the dark matter particle and **its decoupling temperature T_d** are obtained.

The phase-space density today is a factor Z smaller than its primordial value. The **decreasing factor Z > 1** is due to the effect of self-gravity interactions: **the range of Z is computed.**

OBSERVATIONS

The observed dark matter energy density observed today has the value $\rho_{DM} = 0.228 \ (2.518 \ meV)^4$.

In addition, compilation of galaxy observations yield the one dimensional velocity dispersion σ and the radius L in the ranges

$6.6 \ km/s \leq \sigma \leq 11.1 \ km/s$, $\quad 0.5 \ kpc \leq L \leq 1.8 \ kpc$

And the Phase-space Density today (with a precision of a factor 10) has the value :

$D(0) \sim 5 \times 10^3 \ [keV/cm^3] \ (km/s)^{-3} = (0.18 \ keV)^4$.

→**Compilation of observations** of galaxies candidates for DM structure, are compatible with a core of smooth central density and a low mean mass density ~ 0.1 Msun /pc³ rather than with a cusp.

→Dark matter particles can decouple being ultrarelativistic or non-relativistic. Dark matter must be non-relativistic during structure formation in order to reproduce the observed small structure at ~ 2 − 3 kpc.

→In addition, the decoupling can occurs at local thermal equilibrium or out of local thermal equilibrium. All these cases have been considered in our analysis.

RESULTS on DARK MATTER :

(i) the mass of the **dark matter particle is in the keV scale,**T_d **is 100 GeV** at least.

(ii) The **free-streaming length** today is in the **kpc range**, consistent with the observed small scale structure and **the Jean's mass is in the range of the galactic masses, 10^{12} M$_{sun}$.**

(iii) Dark matter **self-interactions** (other than grav.) **are negligible.**

(iv) The **keV scale mass** dark matter determines **cored** (non cusped) dark matter halos.

(v) DM candidates with **typical high masses 100 GeV** ("wimps") **result strongly disfavored**.

keV SCALE DARK MATTER PARTICLES REPRODUCE:

→OBSERVED GALAXY **DENSITIES AND VELOCITY DISPERSIONS**

→OBSERVED GALAXY **DENSITY PROFILES**

->OBSERVED **SURFACE DENSITY** VALUES OF DARK MATTER DOMINATED GALAXIES

Dark Matter

DM particles can decouple being ultrarelativistic (UR) at $T_d \gg m$ or non-relativistic $T_d \ll m$.

We consider particles that decouple at or out of LTE (LTE = local thermal equilibrium).

Distribution function: $F_d[p_c]$ freezes out at decoupling.

p_c = comoving momentum.

$P_f(t) = p_c/a(t)$ = Physical momentum,

Velocity fluctuations: $\qquad\qquad y = P_f(t)/T_d(t) = p_c/T_d$

$$\langle \vec{V}^2(t) \rangle = \langle \frac{\vec{P}_f^2(t)}{m^2} \rangle = \left[\frac{T_d}{m\, a(t)} \right]^2 \frac{\int_0^\infty y^4 F_d(y) dy}{\int_0^\infty y^2 F_d(y) dy} \;.$$

Energy Density: $\rho_{DM}(t) = \frac{m\, g}{2\pi^2} \frac{T_d^3}{a^3(t)} \int_0^\infty y^2 \, F_d(y) \, dy$,

g : # of internal degrees of freedom of the DM particle, $1 \leq g \leq 4$. Formula valid when DM particles are non-relativistic.

The formula for the Mass of the Dark Matter particles

Energy Density: $\rho_{DM}(t) = g \int \frac{d^3 P_f}{(2\pi)^3} \sqrt{m^2 + P_f^2} \, f_d[a(t) \, P_f]$

g : # of internal degrees of freedom of the DM particle, $1 \leq g \leq 4$. For $z \lesssim 30 \Rightarrow$ DM particles are non-relativistic:

$\rho_{DM}(t) = m \, g \, \frac{T_d^3}{a^3(t)} \int_0^\infty y^2 \, f_d(y) \, \frac{dy}{2\pi^2}$.

Using entropy conservation: $\quad T_d = \left(\frac{2}{g_d}\right)^{\frac{1}{3}} T_\gamma \, (1 + z_d)$,

$g_d =$ effective # of UR degrees of freedom at decoupling, $T_\gamma = 0.2348$ meV $\quad , \quad 1 \, \text{meV} = 10^{-3}$ eV.

Today $\Omega_{DM} = \rho_{DM}(0)/\rho_c = 0.105/h^2$ and we obtain for the **mass** of the DM particle:

$m = 6.986 \, \text{eV} \, \dfrac{g_d}{g \displaystyle\int_0^\infty y^2 \, f_d(y) \, dy}$. Goal: determine m and g_d

Dark Matter density and DM velocity dispersion

Energy Density: $\rho_{DM}(t) = g \int \frac{d^3 P_f}{(2\pi)^3} \sqrt{m^2 + P_f^2}\, F_d[a(t)\, P_f]$

g : # of internal degrees of freedom of the DM particle, $1 \leq g \leq 4$. For $z \lesssim 30 \Rightarrow$ DM particles are non-relativistic:

$\rho_{DM}(t) = \frac{m\, g}{2\pi^2} \frac{T_d^3}{a^3(t)} \int_0^\infty y^2\, F_d(y)\, dy$,

Using entropy conservation: $T_d = \left(\frac{2}{g_d}\right)^{\frac{1}{3}} T_{CMB}$,

$g_d =$ effective # of UR degrees of freedom at decoupling, $T_{CMB} = 0.2348\, 10^{-3}$ eV, and

$\rho_{DM}(\text{today}) = \frac{m\, g}{\pi^2\, g_d} T_{CMB}^3 \int_0^\infty y^2\, F_d(y)\, dy = 1.107 \frac{\text{keV}}{\text{cm}^3}$ (1)

We obtain for the primordial velocity dispersion:

$\sigma_{DM}(z) = \sqrt{\frac{1}{3} \langle \vec{V}^2 \rangle (z)} = 0.05124 \frac{1+z}{g_d^{\frac{1}{3}}} \left[\frac{\int_0^\infty y^4\, F_d(y)\, dy}{\int_0^\infty y^2\, F_d(y)\, dy} \right]^{\frac{1}{2}} \frac{\text{keV}}{m} \frac{\text{km}}{\text{s}}$

Goal: determine m and g_d. We need TWO constraints.

Phase-space density invariant under universe expansion

Using again entropy conservation to replace T_d yields for the one-dimensional velocity dispersion,

$$\sigma_{DM}(z) = \sqrt{\frac{1}{3}\langle \vec{V}^2\rangle(z)} = \frac{2^{\frac{1}{3}}}{\sqrt{3}}\frac{1+z}{g_d^{\frac{1}{3}}}\frac{T_\gamma}{m}\sqrt{\frac{\int_0^\infty y^4\, F_d(y)\, dy}{\int_0^\infty y^2\, F_d(y)\, dy}} =$$

$$= 0.05124\,\frac{1+z}{g_d^{\frac{1}{3}}}\,\frac{\text{keV}}{m}\left[\frac{\int_0^\infty y^4\, F_d(y)\, dy}{\int_0^\infty y^2\, F_d(y)\, dy}\right]^{\frac{1}{2}}\frac{\text{km}}{\text{s}}.$$

Phase-space density: $\mathcal{D} \equiv \dfrac{n(t)}{\langle \vec{P}^2_{phys}(t)\rangle^{\frac{3}{2}}} \overset{\text{non}-\text{rel}}{=} \dfrac{\rho_{DM}}{3\sqrt{3}\,m^4\,\sigma_{DM}^3}$

$\mathcal{D}$ is computed theoretically from freezed-out distributions:

$$\mathcal{D} = \frac{g}{2\,\pi^2}\frac{\left[\int_0^\infty y^2 F_d(y)dy\right]^{\frac{5}{2}}}{\left[\int_0^\infty y^4 F_d(y)dy\right]^{\frac{3}{2}}}$$

Theorem: The phase-space density $\mathcal{D}$ can only decrease under self-gravity interactions (gravitational clustering) [Lynden-Bell, Tremaine, Henon, 1986].

The phase-space density $Q \equiv \rho/\sigma^3$ is invariant under the cosmological expansion and can only decrease under self-gravity interactions (gravitational clustering).

The phase-space density today follows observing dwarf spheroidal satellite galaxies of the Milky Way (dSphs)

$$\frac{\rho_s}{\sigma_s^3} \sim 5 \times 10^3 \, \frac{\text{keV/cm}^3}{(\text{km/s})^3} = (0.18 \, \text{keV})^4 \quad \text{Gilmore et al. 07 and 08.}$$

During structure formation $(z \lesssim 30)$, $Q = \rho/\sigma^3$ decreases by a factor that we call Z:

$$Q_{today} = \frac{1}{Z} \, Q_{prim} \quad , \quad Q_{prim} = \frac{\rho_{prim}}{\sigma_{prim}^3} \quad , \quad (2) \quad Z > 1.$$

The spherical model gives $Z \simeq 41000$ and N-body simulations indicate: $10000 > Z > 1$. Z is galaxy dependent.

Constraints: First $\rho_{DM}(\text{today})$, Second $Q_{today} = \rho_s/\sigma_s^3$

Mass Estimates for DM particles

Combining the previous expressions lead to general formulas for m and g_d:

$$m = 0.2504 \, \text{keV} \, \left(\frac{Z}{g}\right)^{\frac{1}{4}} \frac{\left[\int_0^\infty y^4 \, F_d(y) \, dy\right]^{\frac{3}{8}}}{\left[\int_0^\infty y^2 \, F_d(y) \, dy\right]^{\frac{5}{8}}}$$

$$g_d = 35.96 \, Z^{\frac{1}{4}} \, g^{\frac{3}{4}} \, \left[\int_0^\infty y^4 \, F_d(y) \, dy \, \int_0^\infty y^2 \, F_d(y) \, dy\right]^{\frac{3}{8}}$$

These formulas yield for relics decoupling UR at LTE:

$$m = \left(\frac{Z}{g}\right)^{\frac{1}{4}} \, \text{keV} \begin{cases} 0.568 \\ 0.484 \end{cases}, \, g_d = g^{\frac{3}{4}} \, Z^{\frac{1}{4}} \begin{cases} 155 & \text{Fermions} \\ 180 & \text{Bosons} \end{cases}.$$

Since $g = 1 - 4$, we see that $g_d > 100 \Rightarrow T_d > 100$ GeV.

$1 < Z^{\frac{1}{4}} < 5.6$ for $1 < Z < 1000$. Example: for DM Majorana fermions $(g = 2)$ $m \simeq 0.85$ keV.

Mass Estimates for DM particles

Constraints: First $\rho_{DM}(\text{today})$, Second $Q_{today} = \rho_s/\sigma_s^3$

Combining the previous expressions lead to general formulas for m and g_d:

$$m = \frac{2^{\frac{1}{4}}\sqrt{\pi}}{3^{\frac{3}{8}} g^{\frac{1}{4}}} \; Z^{\frac{1}{4}} \; Q_{today}^{\frac{1}{4}} \; \frac{I_4^{\frac{3}{8}}}{I_2^{\frac{5}{8}}} \;\; , \;\; g_d = \frac{2^{\frac{1}{4}} g^{\frac{3}{4}}}{3^{\frac{3}{8}} \pi^{\frac{3}{2}} \Omega_{DM}} \; \frac{T_\gamma^3}{\rho_c} \; Q_{today}^{\frac{1}{4}} \; Z^{\frac{1}{4}} \; [I_2 \, I_4]^{\frac{3}{8}}$$

where: $Q_{today}^{\frac{1}{4}} = 0.18$ keV from the dSphs data,

$T_\gamma = 0.2348$ meV , $\Omega_{DM} = 0.228$, $\rho_c = (2.36 \text{ meV})^4$

These formulas yield for relics decoupling UR at LTE:

$$m = \left(\frac{Z}{g}\right)^{\frac{1}{4}} \text{ keV} \begin{cases} 0.568 \\ 0.484 \end{cases} , \; g_d = g^{\frac{3}{4}} Z^{\frac{1}{4}} \begin{cases} 155 & \text{Fermions} \\ 180 & \text{Bosons} \end{cases} .$$

Since $g = 1 - 4$, we see that $g_d \gtrsim 100 \Rightarrow T_d \gtrsim 100$ GeV.

$1 < Z^{\frac{1}{4}} < 10$ for $1 < Z < 10000$. Example: for DM Majorana fermions $(g = 2)$ 0.5 keV $\lesssim m \lesssim 5$ keV.

Out of thermal equilibrium decoupling

Results for m and g_d on the same scales for DM particles decoupling UR out of thermal equilibrium.

For the χ model of sterile neutrinos where decoupling is out of thermal equilibrium:

$$0.56\,\text{keV} \lesssim m_\nu \, Z^{-\frac{1}{4}} \lesssim 1.0\,\text{keV} \quad , \quad 15 \lesssim g_d \, Z^{-\frac{1}{4}} \lesssim 84$$

Therefore, $0.6\,\text{keV} \lesssim m_\nu \lesssim 10\,\text{keV} \quad , \quad 20 \lesssim g_d \lesssim 850$.

Relics decoupling non-relativistic:
similar bounds: $\text{keV} \lesssim m \lesssim \text{MeV}$

D. Boyanovsky, H. J. de Vega, N. Sanchez,
Phys. Rev. D 77, 043518 (2008), arXiv:0710.5180.

H. J. de Vega, N. G. Sanchez, MNRAS 404, 885 (2010),
arXiv:0901.0922.

Relics decoupling non-relativistic

$$F_d^{NR}(p_c) = \frac{2^{\frac{5}{2}} \pi^{\frac{7}{2}}}{45} \, g_d \, Y_\infty \, \left(\frac{T_d}{m}\right)^{\frac{3}{2}} \, e^{-\frac{p_c^2}{2\,m\,T_d}} = \frac{2^{\frac{5}{2}} \pi^{\frac{7}{2}}}{45} \, \frac{g_d \, Y_\infty}{x^{\frac{3}{2}}} \, e^{-\frac{y^2}{2\,x}}$$

$Y(t) = n(t)/s(t)$, $n(t)$ number of DM particles per unit volume, $s(t)$ entropy per unit volume, $x \equiv m/T_d$, $T_d < m$.

$Y_\infty = \frac{1}{\pi} \, \sqrt{\frac{45}{8}} \, \frac{1}{\sqrt{g_d} \, T_d \, \sigma_0 \, M_{Pl}}$ late time limit of Boltzmann.

σ_0: thermally averaged total annihilation cross-section times the velocity.

From our general equations for m and g_d:

$$m = \frac{45}{4\,\pi^2} \, \frac{\Omega_{DM} \, \rho_c}{g \, T_\gamma^3 \, Y_\infty} = \frac{0.748}{g \, Y_\infty} \text{ eV} \quad \text{and} \quad m^{\frac{5}{2}} \, T_d^{\frac{3}{2}} = \frac{45}{2\,\pi^2} \, \frac{1}{g \, g_d \, Y_\infty} \, Z \, \frac{\rho_s}{\sigma_s^3}$$

Finally:

$$\sqrt{m\,T_d} = 1.47 \, \left(\frac{Z}{g_d}\right)^{\frac{1}{3}} \text{keV}. \quad m = 3.67 \text{ keV } Z^{\frac{1}{3}} \, \frac{g_d^{\frac{1}{12}}}{\sqrt{g}} \, \sqrt{\frac{\sigma_0}{\text{pb}}}$$

We used ρ_{DM} today and the decrease of the phase space density by a factor Z. 1 pb $= 10^{-36}$ cm$^2 = 0.257$ /(10^5 GeV^2).

Relics decoupling non-relativistic 2

Allowed ranges for m and T_d.

$m > T_d > b$ eV where $b > 1$ or $b \gg 1$ for DM decoupling in the RD era

$$\left(\frac{Z}{g_d}\right)^{\frac{1}{3}} 1.47 \text{ keV} < m < \frac{2.16}{b} \text{ MeV} \left(\frac{Z}{g_d}\right)^{\frac{2}{3}}$$

$g_d \simeq 3$ for $1 \text{ eV} < T_d < 100 \text{ keV}$ and $1 < Z < 10^3$

$1.02 \text{ keV} < m < \frac{104}{b} \text{ MeV}$, $T_d < 10.2$ keV.

Only using ρ_{DM} today (ignoring the phase space density information) gives one equation with three unknowns: m, T_d and σ_0,

$\sigma_0 = 0.16 \text{ pbarn} \dfrac{g}{\sqrt{g_d}} \dfrac{m}{T_d}$ http://pdg.lbl.gov

WIMPS with $m = 100$ GeV and $T_d = 5$ GeV require $Z \sim 10^{23}$.

- **The comoving Jeans' (free-streaming) wavelength,** ie the largest wavevector exhibiting gravitational instability , and **the Jeans' mass** (the smallest unstable mass by gravitational collapse) are obtained in the range

$$0.76 \text{ kpc} / (\sqrt{1 + z}) \; < \; \lambda_{fs}(z) \; < \; 16.3 \text{ kpc} / (\sqrt{1 + z})$$

$$0.45 \; 10^3 \text{ M}_{sun} \; < \text{M}_J (z) (1 + z)^{-3/2} \; < 0.45 \; 10^7 \text{ M}_{sun}$$

- **These values at z = 0 are consistent and of order of the small dark matter structures observed today .**

- **By the beginning of the matter dominated era z ~ 3200, the masses are of the order of galactic masses 10^{12} M$_{sun}$ and the comoving free-streaming length is of the order of the galaxy sizes today ~ 100 kpc**
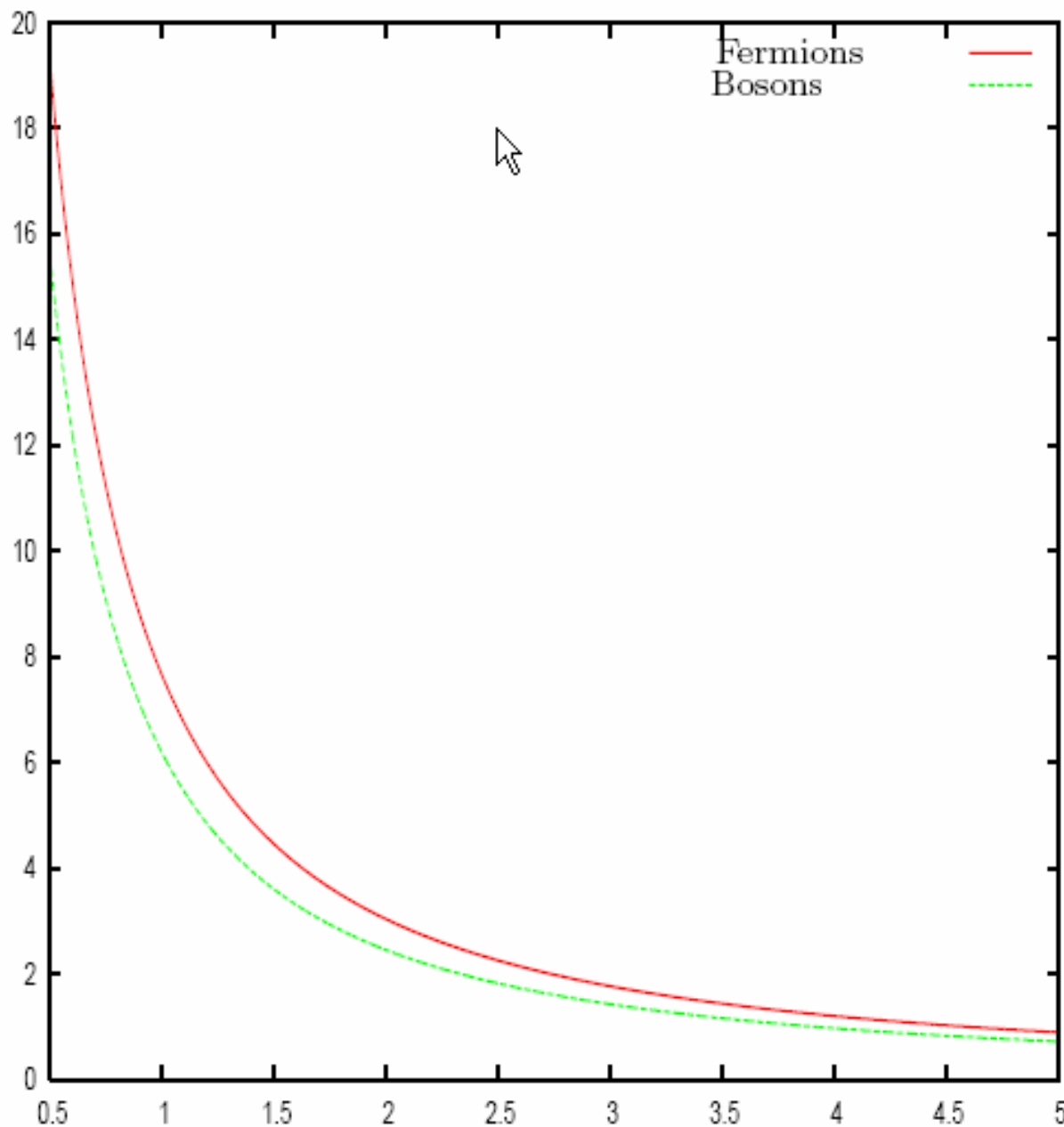
The free-streaming wavelength today in kpc vs. the dark matter particle mass in keV. *It decreases for increasing mass m and shows little variation with the particle*

- The **mass of the dark matter particle,** independent of the particle model, **is in the keV scale** and the **temperature when the dark matter particles decoupled** is in **the 100 GeV scale at least.**

Robust result. No assumption about the particle physics model of the dark matter particle.

keV DM mass much larger than temperature in matter dominated era (which is less than 1 eV)

m and T_d **are mildly affected by the uncertainty in the factor Z** through **a power factor 1/4** of this uncertainty, namely, by a factor $10^{1/4} \sim 1.8.$

- **Lower and upper bounds for the dark matter annihilation cross-section σ_0 are derived: $\sigma_0 > (0.239 - 0.956) \, 10^{-9} \, \text{GeV}^{-2}$ and $\sigma_0 < 3200 \, \text{m} \, \text{GeV}^{-3}$. There is at least five orders of magnitude between them , the dark matter non gravitational self-interaction is negligible** (consistent with structure formation and observations, X-ray, optical and lensing observations of the merging of galaxy clusters).

- **Typical "wimps" (weakly interacting massive particles) with mass m = 100 GeV and T_d = 5 GeV would require a huge $Z \sim 10^{23}$, well above the upper bounds obtained and cannot reproduce the observed galaxy properties.**

**Wimps produce extremely short free-streaming or Jeans length today λ_{fs} (0) = 3.51 10^{-4} pc = 72.4 AU that would correspond to unobserved structures much smaller than the galaxy structure. Wimps result strongly disfavoured. [TOO cold]**

In all cases: DM particles decoupling either ultra-relativistic or non-relativistic, LTE or OTE :

(i) the mass of the **dark matter particle is in the keV scale**, T_d is 100 GeV at least.

(ii) The **free-streaming length** today is in the **kpc range**, consistent with the observed small scale structure and the Jean's mass is in the range of the galactic masses, $10^{12} M_{sun}$.

(iii) Dark matter **self-interactions** (other than grav.) **are negligible.**

(iv) The **keV scale mass** dark matter determines **cored** (non cusped) dark matter halos.

(v) DM candidates with typical high masses 100 GeV ("wimps") **result strongly disfavored**.

Linear primordial power today $P(k)$ vs. k Mpc h
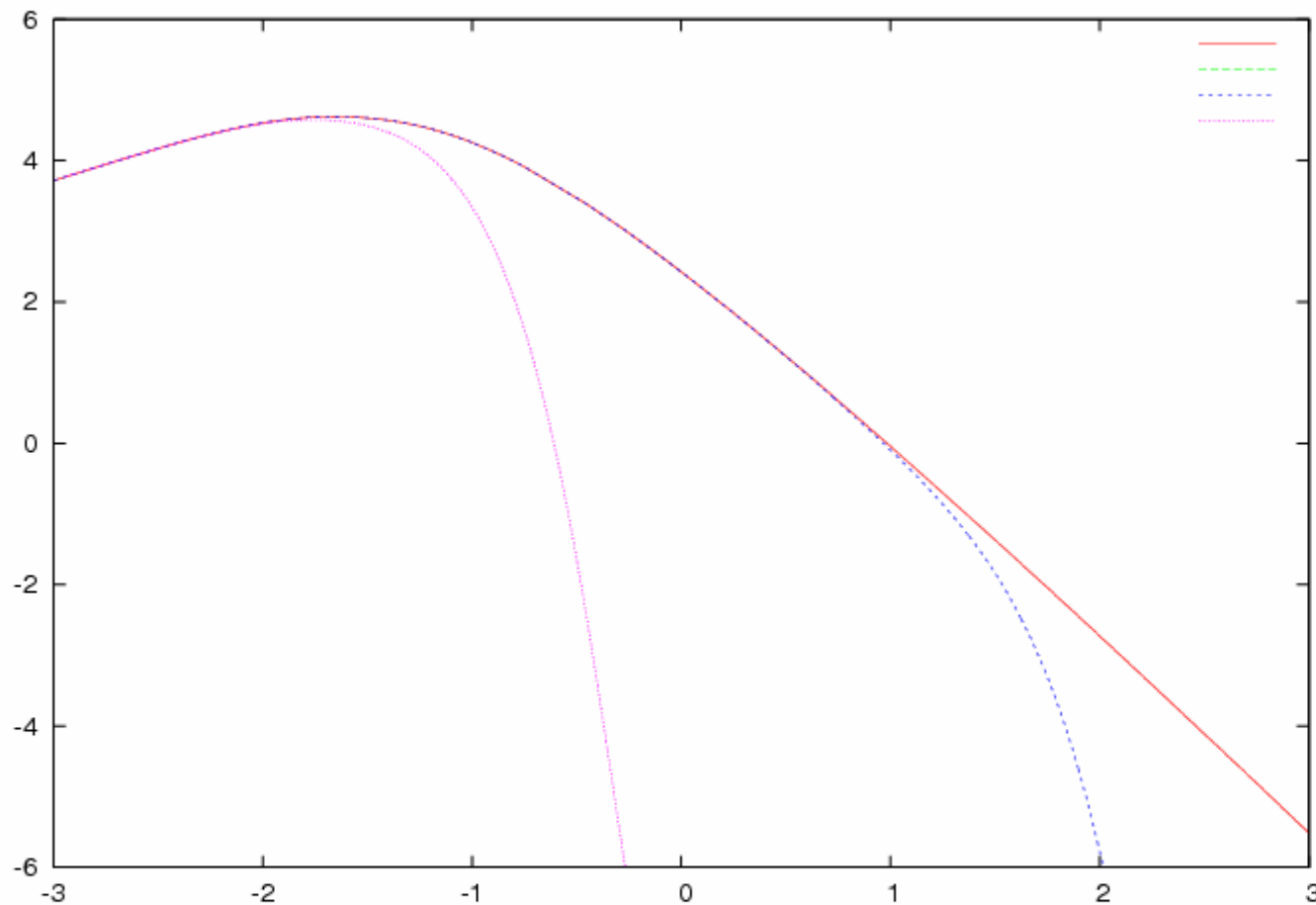
$\log_{10} P(k)$ vs. $\log_{10}[k \text{ Mpc } h]$ for **WIMPS**, 1 keV DM particles and 10 eV DM particles. $P(k) = P_0 \, k^{n_s} \, T^2(k)$.

$P(k)$ cutted for 1 keV DM particles on scales $\lesssim 100$ kpc.

Transfer function in the MD era from Gilbert integral eq
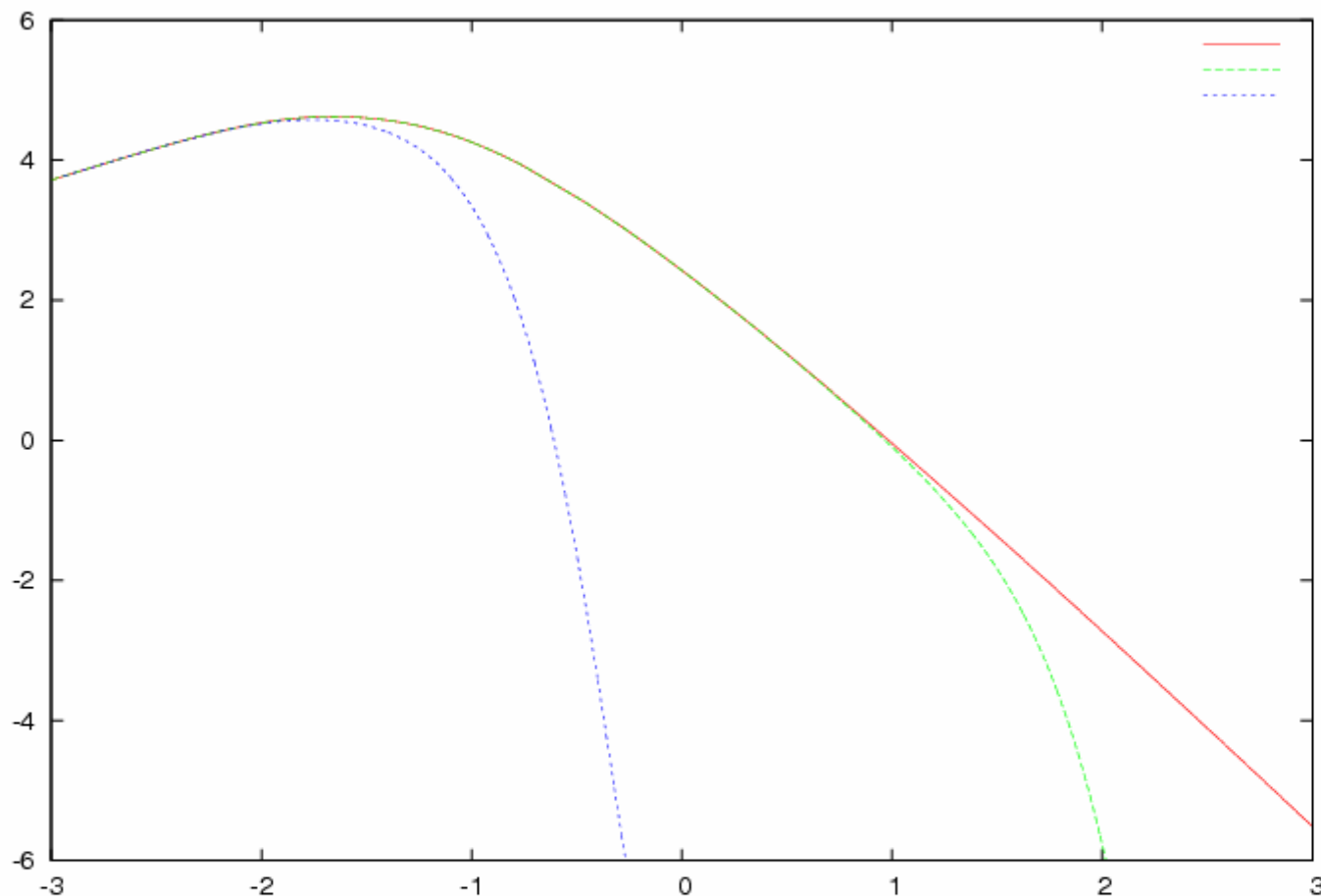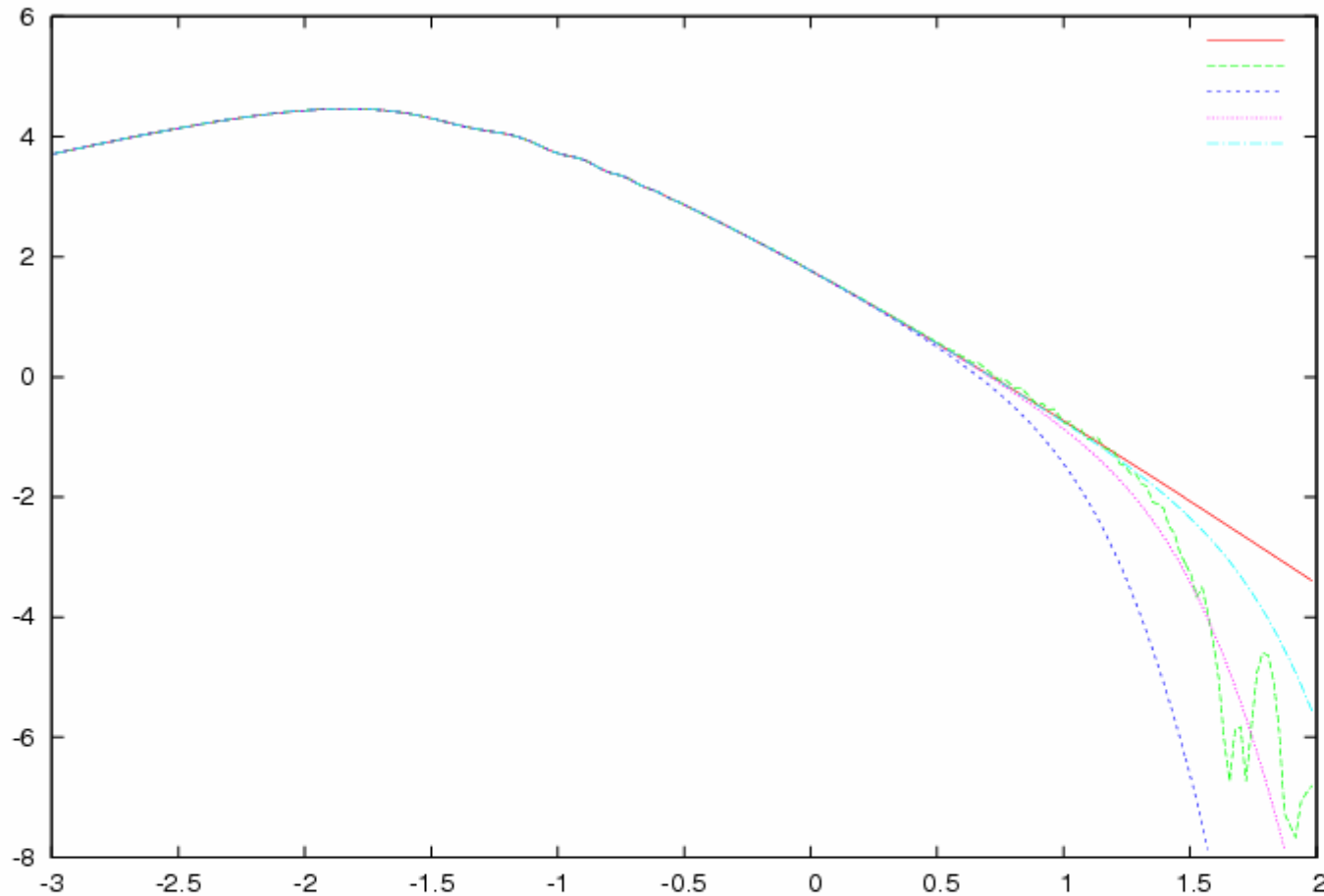
Linear primordial power today $P(k)$ vs. k Mpc h

$\log_{10} P(k)$ vs. $\log_{10}[k \text{ Mpc } h]$ for **WIMPS**, 1 keV DM particles and 10 eV DM particles. $P(k) = P_0 \; k^{n_s} \; T^2(k)$.

$P(k)$ cutted for 1 keV DM particles for scales < 100 kpc.

Transfer function in the MD era from Gilbert integral eq.
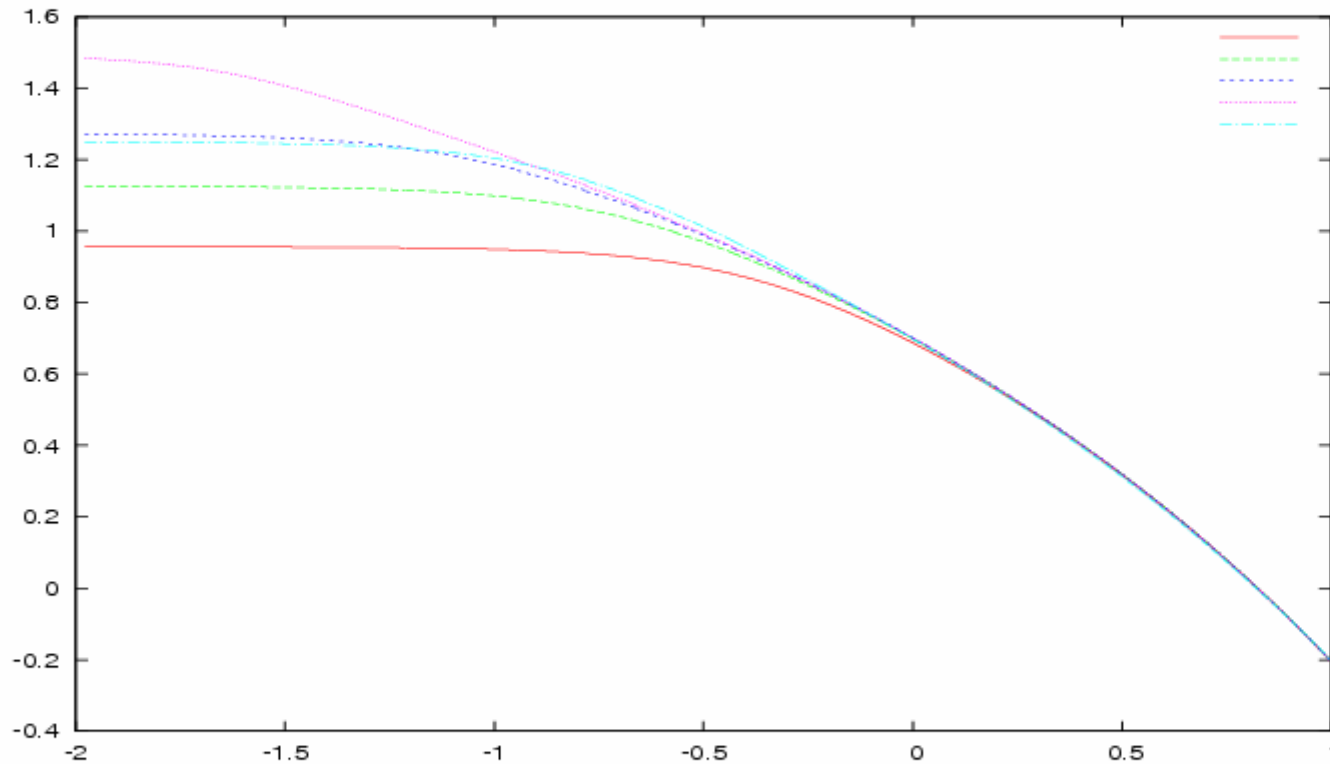
Linear primordial power today $P(k)$ **vs.** k **Mpc** h

$\log_{10} P(k)$ vs. $\log_{10}[k \text{ Mpc } h]$ for CDM, 1 keV, 2 keV, light-blue 4 keV DM particles decoupling in equil, and 1 keV sterile neutrinos. WDM cuts $P(k)$ on small scales

$$r \lesssim 100 \, (\text{keV}/m)^{4/3} \text{ kpc}$$

The expected overdensity

The expected overdensity within a radius R in the linear regime

$$\sigma^2(R) = \int_0^\infty \frac{dk}{k} \, \Delta^2(k) \, W^2(kR) \quad , \quad W(kR) : \text{window function.}$$

$\log \sigma(R)$ vs. $\log R$ for CDM, 1 keV, 2 keV, 4 keV DM particles decoupling in equil, and 1 keV (light-blue) sterile neutrinos. WDM flattens and reduces $\sigma(R)$ for small scales.

Linear and non-linear regimes in z and R

$\sigma^2(R,z) \sim 1$: borderline between linear and non-linear regimes. Objects (galaxies) of scale R and mass $\sim R^3$ start to form when this scale becomes non-linear.
Smaller objects form earlier.
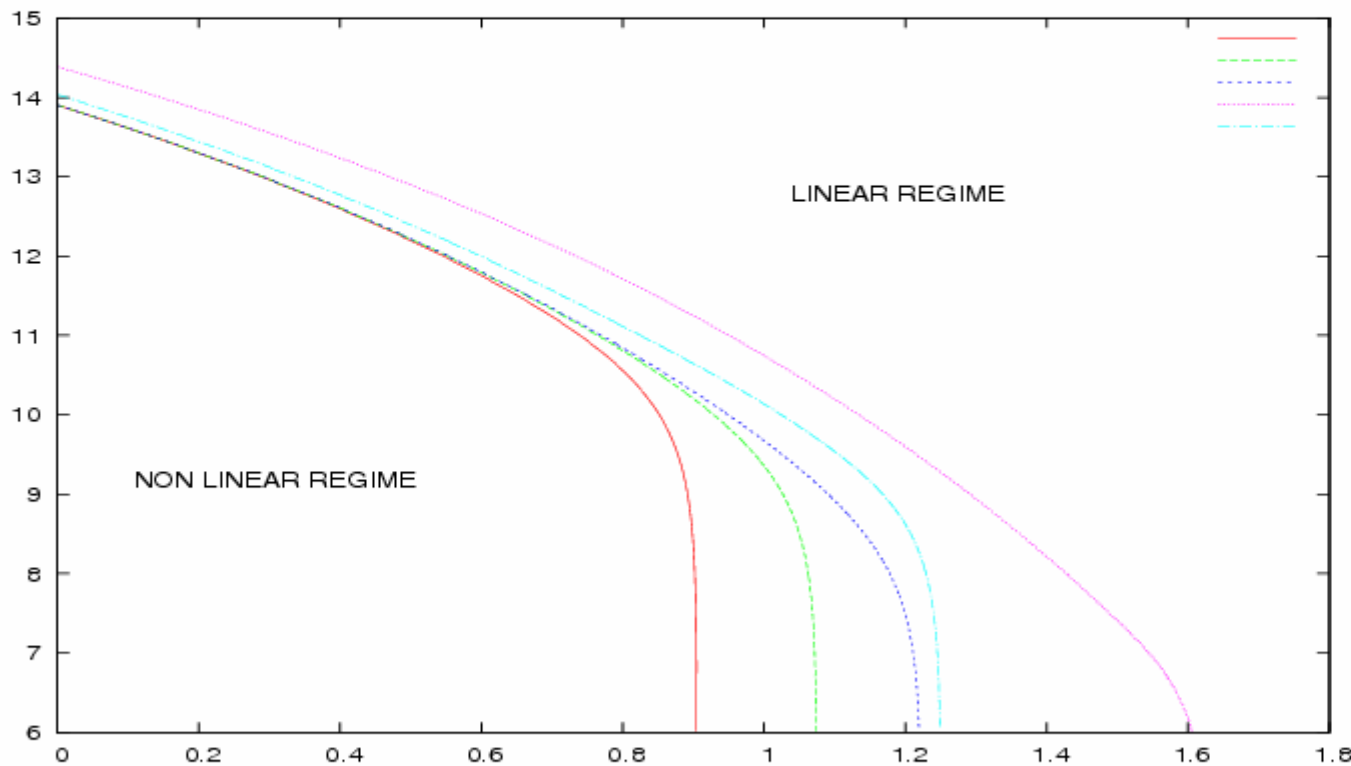
$\log M/M_\odot$ vs. $\log(z+1)$ for CDM, 1 keV, 2 keV, 4 keV DM particles decoupling in equil, and 1 keV (light-blue) sterile ν.

WDM properties

WDM is characterized by

- its initial power spectrum cutted off for scales below ~ 50 kpc. Thus, structures are not formed in WDM for scales below ~ 50 kpc.

- its initial velocity dispersion.

Both features are crucial in structure formation.

N-body simulations show that structure formation happens slower in WDM than in CDM mainly due to the velocity dispersion of the WDM particles.

Structure formation is hierarchical in CDM.

WDM simulations show in addition top-hat structure formation at small scales and high densities but hierarchical structure formation remains dominant, especially at large scales and low densities.

Kinetic Theory in Cosmology

Distribution function in phase-space: $f(t, p_i, x^i)$, $i = 1, 2, 3$

Boltzmann-Vlasov equation:

$$\frac{df}{dt} = \frac{\partial f}{\partial t} + \frac{p^i}{p^0} \frac{\partial f}{\partial x^i} + \frac{dp_i}{dt} \frac{\partial f}{\partial p_i} = \text{Collision terms}$$

Geodesic equations:

$$\frac{dx^\alpha}{dt} = \frac{p^\alpha}{p^0} \quad , \quad \frac{dp_\alpha}{dt} = -\frac{1}{2\, p^0}\, p_\beta\, p_\gamma \frac{\partial g^{\beta\gamma}}{\partial x^\alpha} \quad , \quad 0 \le \alpha, \beta, \gamma \le 3$$

The Einstein equations determine the metric $g_{\alpha\beta}(t, x^i)$ in terms of the matter+radiation distribution function given by $f(t, p_i, x^i) \Rightarrow$ the Boltzmann-Vlasov equation becomes non-linear.

Collision terms negligible after particle decoupling.

The Boltzmann-Vlasov equation can be linearized around the FRW cosmological geometry before structure formation.

Galaxies

Physical variables in galaxies:

a) Nonuniversal quantities: mass, size, luminosity, fraction of DM, DM core radius r_0, central DM density ρ_0, ...

b) Universal quantities: surface density $\mu_0 \equiv r_0 \, \rho_0$ and DM density profiles. M_{BH}/M_{halo} (or the halo binding energy).

The galaxy variables are related by universal empirical relations. Only one variable remains free.

Universal quantities may be attractors in the dynamical evolution.

Universal DM density profile in Galaxies:

$$\rho(r) = \rho_0 \, F\left(\frac{r}{r_0}\right) \; , \; F(0) = 1 \; , \; x \equiv \frac{r}{r_0} \; , \; r_0 = \text{DM core radius.}$$

Empirical cored profiles: $F_{Burkert}(x) = \frac{1}{(1+x)(1+x^2)}$.

Cored profiles do reproduce the astronomical observations.

The constant surface density in DM and luminous galaxies

The Surface density for dark matter (DM) halos and for luminous matter galaxies defined as: $\mu_{0D} \equiv r_0 \, \rho_0,$

$r_0 =$ halo core radius, $\rho_0 =$ central density for DM galaxies

$$\mu_{0D} \simeq 120 \, \frac{M_\odot}{\mathrm{pc}^2} = 5500 \, (\mathrm{MeV})^3 = (17.6 \, \mathrm{Mev})^3$$

5 kpc $< r_0 <$ 100 kpc. For luminous galaxies $\rho_0 = \rho(r_0)$. Donato et al. 09, Gentile et al. 09.$[\mu_{0D} = g$ in the surface].

Universal value for μ_{0D}: independent of galaxy luminosity for a large number of galactic systems (spirals, dwarf irregular and spheroidals, elliptics) spanning over 14 magnitudes in luminosity and of different Hubble types.

Similar values $\mu_{0D} \simeq 80 \, \frac{M_\odot}{\mathrm{pc}^2}$ in interstellar molecular clouds of size r_0 of different type and composition over scales $0.001 \, \mathrm{pc} < r_0 < 100$ pc (Larson laws, 1981).

Scaling of the energy and entropy from the surface density

Total energy using the virial and the profile $F(x)$:

$$E = \frac{1}{2} \langle U \rangle = -\frac{1}{4} G \int \frac{d^3r \, d^3r'}{|\boldsymbol{r} - \boldsymbol{r}'|} \langle \rho(r) \, \rho(r') \rangle =$$

$$= -\frac{1}{4} G \, \rho_0^2 \, r_0^5 \int \frac{d^3x \, d^3x'}{|\boldsymbol{x} - \boldsymbol{x}'|} \langle F(x) \, F(x') \rangle \quad \Rightarrow \quad E \sim G \, \mu_{0D}^2 \, r_0^3$$

The energy scales as the volume.

For consistency with the profile, the Boltzmann-Vlasov distribution function must scale as

$$f(\boldsymbol{p}, \boldsymbol{r}) = \frac{1}{m^4 \, r_0^3 \, G^{\frac{3}{2}} \, \sqrt{\rho_0}} \, \mathcal{F} \left(\frac{\boldsymbol{p}}{m \, r_0 \, \sqrt{G \, \rho_0}}, \frac{\boldsymbol{r}}{r_0} \right)$$

Hence, the entropy scales as

$$S = \int f(\boldsymbol{p}, \boldsymbol{r}) \, \log f(\boldsymbol{p}, \boldsymbol{r}) \, d^3p \, d^3r \sim r_0^3 \, \frac{\rho_0}{m} = r_0^2 \, \frac{\mu_{0D}}{m} \, .$$

The entropy scales as the surface (as for black-holes).
However, very different proportionality coefficients:

$$\frac{S_{BH}/A}{S_{gal}/r_0^2} \sim \frac{m}{\text{keV}} \, 10^{36} \quad \Rightarrow \text{Much smaller coefficient for galaxies}$$

than for black-holes. Bekenstein bound satisfied.

DM surface density from linear Boltzmann-Vlasov eq

The distribution function of the decoupled DM particles:

$$f(\vec{x}, \vec{p}; t) = g\, f_0^{DM}(p) + F_1(\vec{x}, \vec{p}; t) \quad , \quad f_0^{DM}(p) = \text{zeroth order}$$

DM distribution function in or out of thermal equilibrium.

We evolve the distribution function $F_1(\vec{x}, \vec{p}; t)$ according to the linearized Boltzmann-Vlasov equation since the end of inflation. The DM density fluctuations are given by

$$\Delta(t, \vec{k}) \equiv m \int \frac{d^3p}{(2\pi)^3} \int d^3x \, e^{-i\,\vec{x}\cdot\vec{k}} \, F_1(\vec{x}, \vec{p}; t)$$

Today: $\Delta(\text{today}, \vec{k}) = \rho_{DM}\, \bar{\Delta}(z = 0, k)\, \sqrt{V}\, |\phi_k|\, g(\vec{k})$,

where $\bar{\Delta}(z, k)$ obeys a Volterra integral equation,
the primordial inflationary fluctuations are:

$$|\phi_k| = \sqrt{2}\, \pi\, \frac{|\Delta_0|}{k^{\frac{3}{2}}} \left(\frac{k}{k_0}\right)^{\frac{n_s - 1}{2}} \quad , \quad g(\vec{k}) \text{ is a random gaussian field,}$$

$V = $ phase-space volume at horizon re-entering

$|\Delta_0| \simeq 4.94\ 10^{-5}$, $n_s \simeq 0.964$, $k_0 = 2\ \text{Gpc}^{-1}$, WMAP7 .

Linear density fluctuations today

The linearized Boltzmann-Vlasov equation can be recasted as a Volterra integral equation for the DM density fluctuations:

$\bar{\Delta}(z, k) =$

$h(z, k) + \frac{6}{(z+1) \, k \, r_{lin}} \, \int_{s_0}^{s} ds' \, \Pi\{k \, r_{lin}[s(z) - s']\} \, \bar{\Delta}(z(s'), k)$

$z(s) + 1 = (z_{eq} + 1) \, \sinh^2 s, \; z_{eq} + 1 \simeq 3200, \; \bar{\Delta}(\text{initial}, k) = 1$

$h(z, k) =$ known function: contains the memory from previous UR evolution and the photons gravitational potential.

$\Pi(x) \equiv \int_0^{\infty} Q \, dQ \, f_0^{DM}(Q) \, \sin(Q \, x)$,

$f_0^{DM}(Q) =$ zeroth order freezed-out DM distribution.

This integral equation is valid both in the RD and MD eras as long as the DM particles are non relativistic. It becomes the Gilbert equation in the MD era (plus memory terms).

The Free Streaming Scale

The characteristic length scale is the free streaming scale (or Jeans' scale)

$$r_{lin} = 2\sqrt{1+z_{eq}}\left(\frac{3\,M_{Pl}^2}{H_0\,\sqrt{\Omega_{DM}\,Q_{prim}}}\right)^{\frac{1}{3}} = 21.1\,q_p^{\frac{1}{3}}\ \text{kpc}$$

$q_p \equiv Q_{prim}/(\text{keV})^4$. DM particles can freely propagate over distances of the order of the free streaming scale.
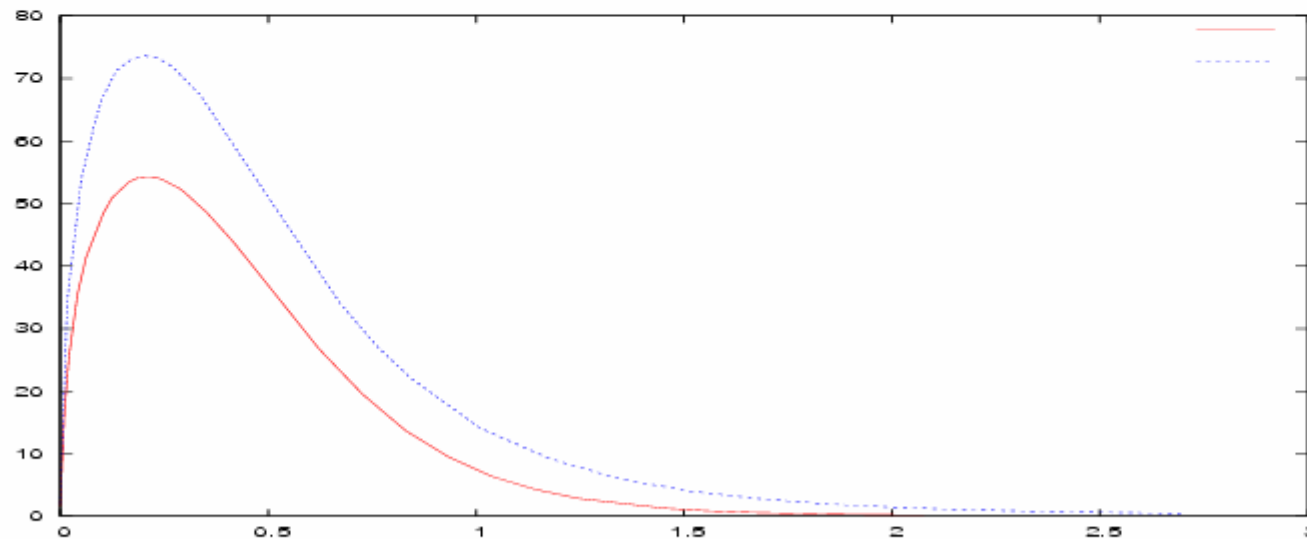
DM fluctuations today $\bar{\Delta}(z=0,k)$ vs. $k\,r_{lin}$. Red= thermal FD initial. Blue = χ-sterile neutrinos. Initial value $\bar{\Delta}(k) = 1$.

Linear density profile today

The matter density fluctuations $\rho_{lin}(r)$ are given today by

$$\rho_{lin}(r) = \frac{1}{2\pi^2 r} \int_0^\infty k \, dk \, \sin(k\,r) \, \Delta(k, t_{\text{today}}) \text{ for } g(\vec{k}) = 1$$

The linear profile today results:

$$\rho_{lin}(x) = 14.47 \, \rho_{DM} \, \frac{q_p^{\frac{n_s+2}{3}}}{x} \, \frac{I_3}{[(z_i+1)(z_i+1+z_{eq})]^{\frac{3}{4}}} \times$$

$$\times \int_0^\infty \gamma^{n_s/2-1} \, d\gamma \, \sin(\gamma \, x) \, \bar{\Delta}(z = 0, \gamma)$$
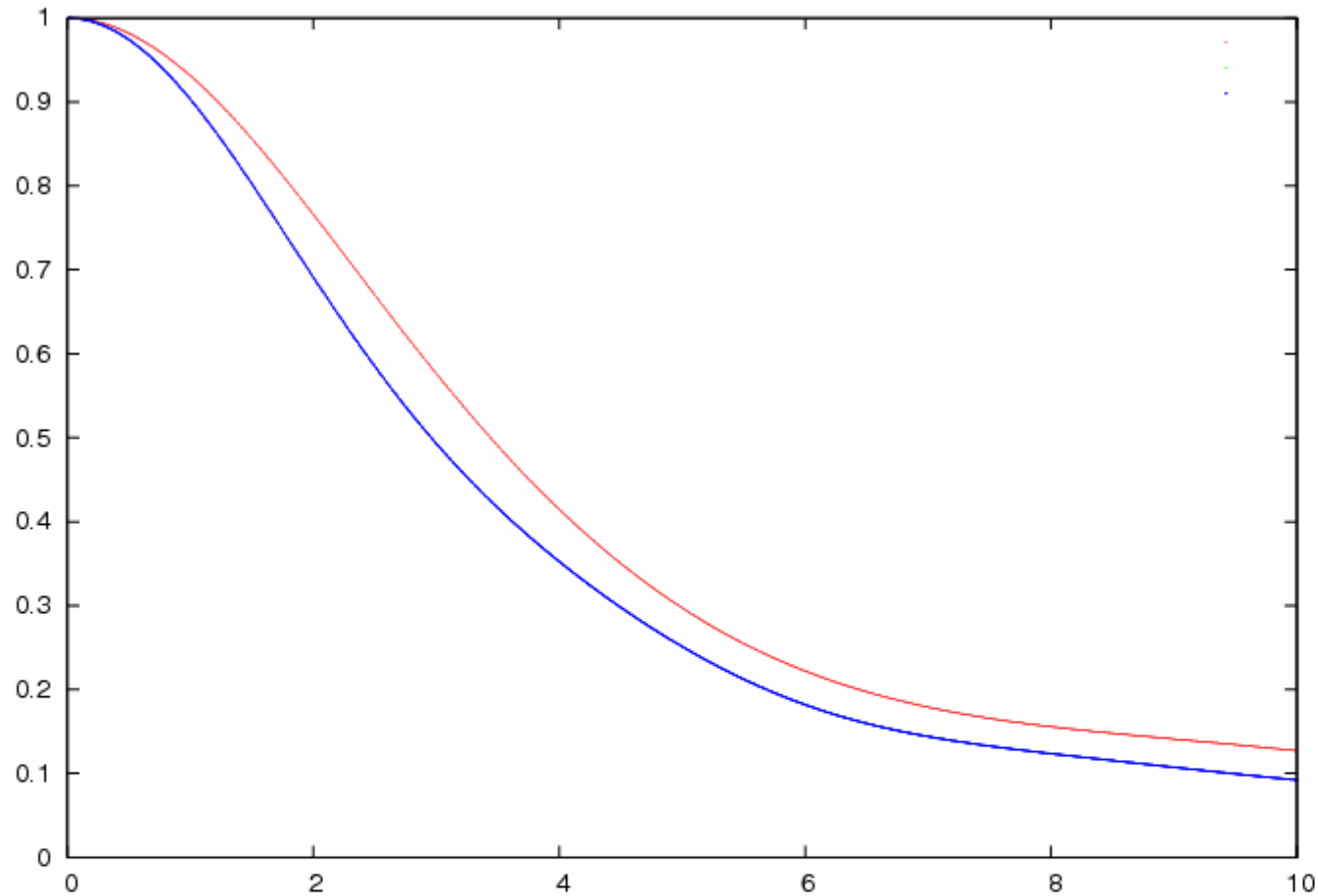
where $\gamma \equiv k \, r_{lin}$ and $x \equiv r/r_{lin}$.

I_n and $\bar{\Delta}(z = 0, \gamma)$ depend on the freezed-out DM distribution $f_0^{DM}(Q)$.

Phase-space volume at horizon re-entering by redshift

$$z_i : \quad V = \frac{4}{3}\pi \left(\frac{2\pi}{k_i}\right)^3 \quad , \quad k_i = H_0 \sqrt{\Omega_m \, (z_i + 1)(1 + \frac{z_i+1}{z_{eq}+1})}$$

Density profiles in the linear approximation

Profiles $\rho_{lin}(r)/\rho_{lin}(0)$ vs. $x \equiv r/r_{lin}$.

Fermions decoupling ultrarelativistically in and out of thermal equilibrium. The halo radius r_0 is proportional to r_{lin}: $r_0 = \beta\, r_{lin}$. $\beta_{in\,equil} = 5.565$, $\beta_{out\,equil} = 5.013$.

Matching the observed and the theoretical surface density

Theoretical results:

$$m/\text{keV} = q_p^{\frac{1}{4}} \begin{cases} 2.646 \ \text{Thermal Fermi} - \text{Dirac}, \\ 3.144 < 2.418 \, \tau^{-\frac{1}{4}} < 5.591 \ \chi - \text{sterile} \ \nu, \end{cases}$$

$[0.035 < \tau < 0.35$: coupling in the χ sterile neutrino model.$]$

$$m/\text{keV} = q_p^{\frac{1}{3}} \, 10.447 \ , \quad \text{DW model sterile} \ \nu.$$

Surface density: $\mu_0 \equiv r_0 \, \rho(0)$ where $r_0 =$ core radius.

$$\frac{\mu_{0\,lin}}{(\text{MeV})^3} = \left(\frac{m}{\text{keV}}\right)^{\frac{2}{3} n_s} \frac{\mathcal{N}}{N^{\frac{3}{4}}(z_i)} \times \begin{cases} 0.2393 \ \text{Thermal FD} \\ 0.2535 \, \tau^{n_s/6} \chi - \text{sterile} \ \nu, \end{cases}$$

$$\mathcal{N} = \beta \, I_3 \, \int_0^\infty \gamma^{n_s/2} \, d\gamma \, \bar{\Delta}(\text{today}, \gamma) = \begin{cases} 348.4 \ \text{Thermal FD} \\ 383.7 \ \chi - \text{sterile} \ \nu, \end{cases}$$

$n_s = 0.964$ primordial spectral index,

$N(z_i) \equiv (z_i + 1)(z_i + 1 + z_{eq})$.

The DM particle mass m from the observed surface density

Matching the observed values $\mu_{0\,obs}$ with this $\mu_{0\,lin}$ gives q_p, the mass of the DM particle and g_d.

From spiral galaxies data: $\mu_{0\,obs} = 6000\ (\text{MeV})^3$ and the DM particle mass results,

$$\frac{m}{\text{keV}} = \left[\frac{N(z_i)}{N(100)}\right]^{\frac{9}{8\,n_s}} \times \begin{cases} 5.382\ \text{Fermi} - \text{Dirac} \\ 3.07 < 2.36\ \tau^{-\frac{1}{4}} < 5.46\ \chi - \text{sterile}\,\nu, \end{cases}$$

$$\frac{m}{\text{keV}} = 10.8\ \left[\frac{N(z_i)}{N(100)}\right]^{\frac{3}{2\,n_s}}, \quad \text{DW model sterile } \nu.$$

$$N(z_i) \equiv (z_i + 1)(z_i + 1 + z_{eq})$$

UR degrees of freedom ($\Rightarrow$ temperature) at decoupling

$$g_d = \left[\frac{N(100)}{N(z_i)}\right]^{\frac{3}{2\,n_s}} \times \begin{cases} 3293\ \text{Fermi} - \text{Dirac}, \\ 91 < 1124\ \tau^{\frac{3}{4}} < 512\ \chi - \text{sterile}\,\nu, \end{cases}$$

$$g_d = 22.2\ \text{DW model sterile } \nu.$$

Density profiles in the linear approximation

Density profiles turn to be cored at scales $r \ll r_{lin}$.

Intermediate regime $r \gtrsim r_{lin}$:

$$\rho_{lin}(r) \overset{r \gtrsim r_{lin}}{=} c_0 \left(\frac{r_{lin}}{r}\right)^{1+n_s/2} \rho_{lin}(0) \quad , \quad 1 + n_s/2 = 1.482.$$

$\rho_{lin}(r)$ scales with the primordial spectral index n_s.

The theoretical linear results agree with the universal empirical behaviour $r^{-1.6 \pm 0.4}$: M. G. Walker et al. (2009) (observations), I. M. Vass et al. (2009) (simulations).

The agreement between the linear theory and the observations is remarkable.

In the asymptotic regime $r \gg r_{lin}$ the small k behaviour of $\Delta(k, t_{\text{today}}) \overset{k \to 0}{=} c_1 (k\, r_{lin})^s$ with $s \simeq 0.5$ implies the presence of a tail: $\quad \rho_{lin}(r) \overset{r \gg r_{lin}}{\simeq} c \left(\frac{r_{lin}}{r}\right)^2.$
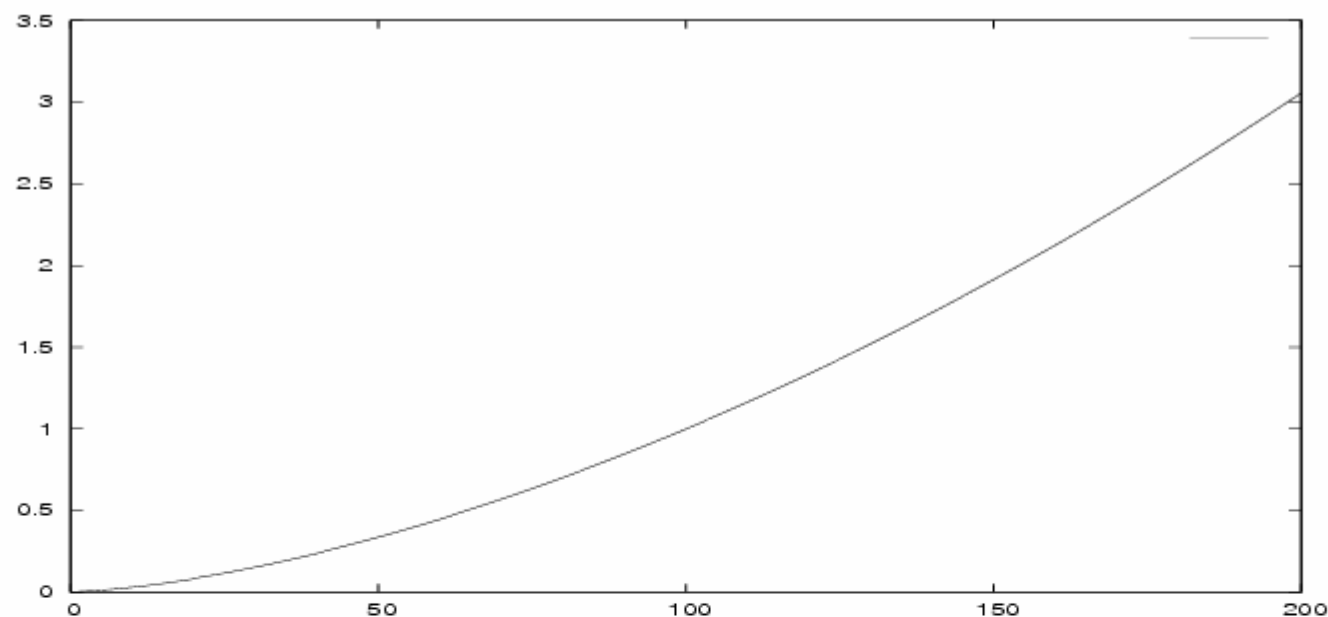
The factor $[N(z_i)/N(100)]^{\frac{3}{2\,n_s}}$ vs. z_i.

Further work:

- Effects of the random initial field $g(\vec{k})$

- Cluster of galaxies where observations indicate a surface density about eight times larger than in galaxies (Salucci et al. in preparation). This factor eight can be explained theoretically by $z_i^{galaxies} \simeq 16\ z_i^{clusters}$.
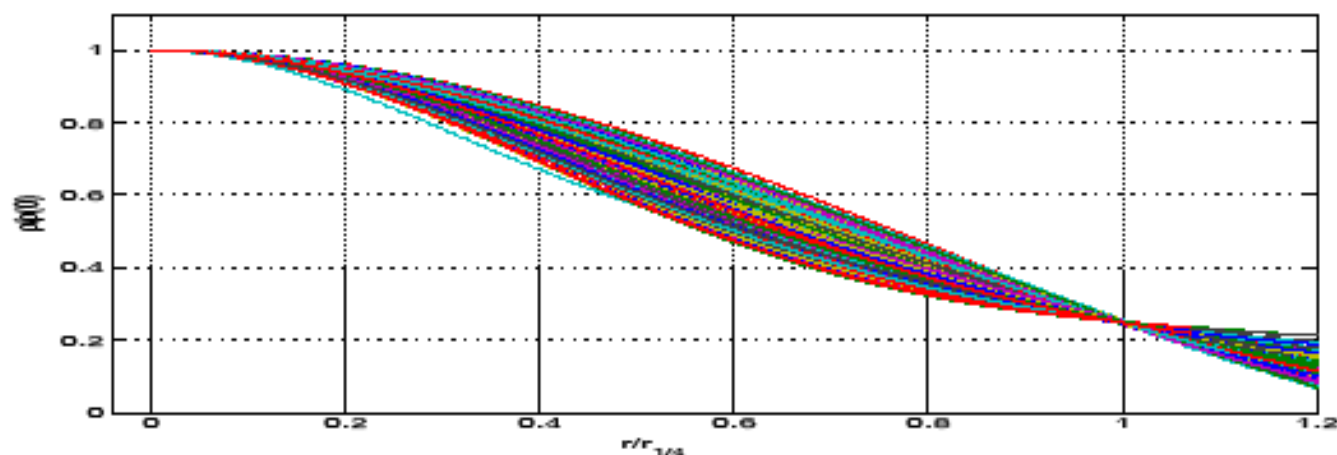
Wimps vs. galaxy observations

	Observed Values	Wimps in linear theory
r_0	5 to 52 kpc	0.045 pc
ρ_0	1.57 to $19.3 \times 10^{-25} \; \frac{\text{g}}{\text{cm}^3}$	$0.73 \times 10^{-14} \; \frac{\text{g}}{\text{cm}^3}$
$\sqrt{\overline{v^2}}_{halo}$	79.3 to 261 km/sec	0.243 km/sec

The wimps values strongly disagree by several order of magnitude with the observations.
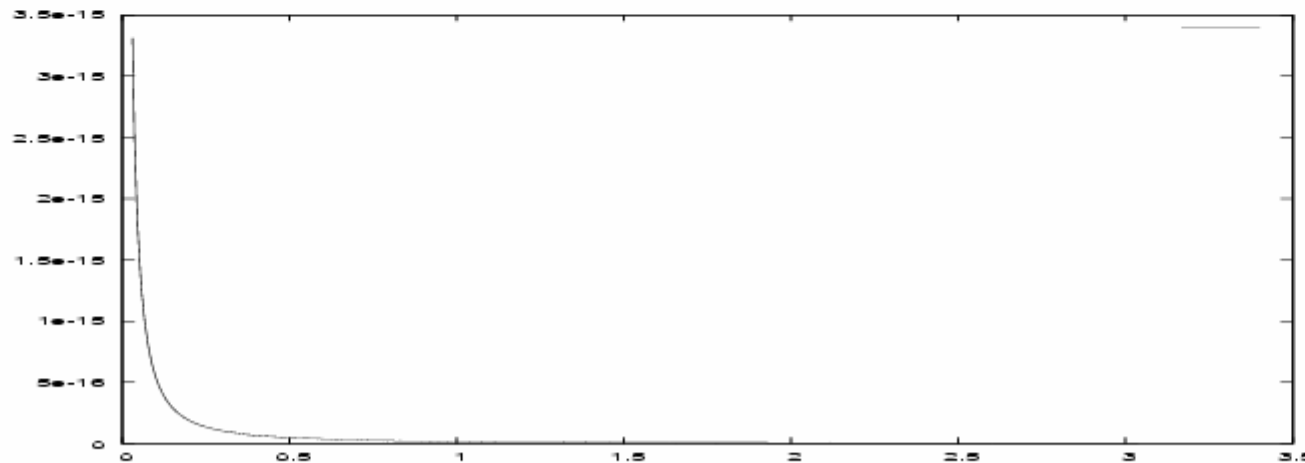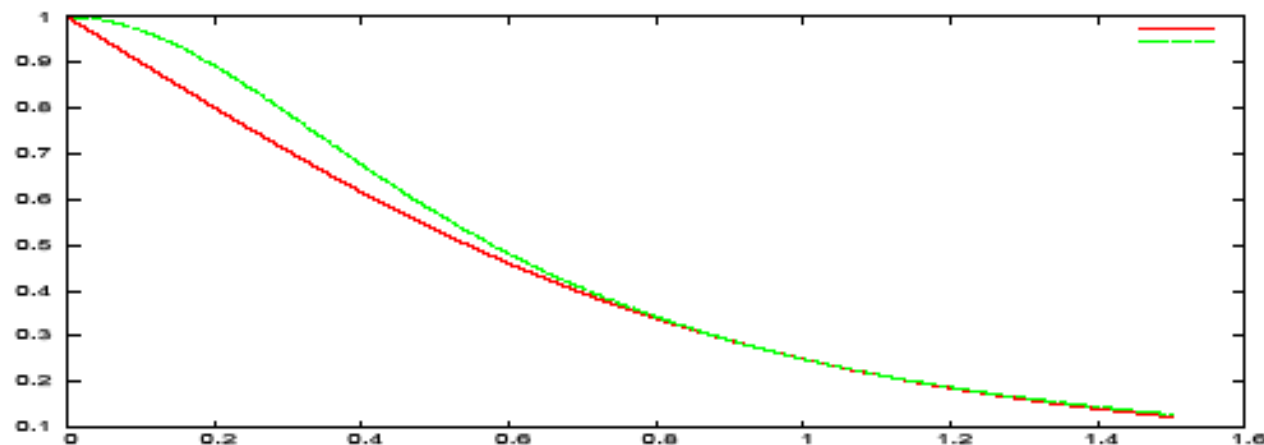

$\rho_{lin}(r)_{wimp}$ in g/cm^3 vs. r in pc. Exhibits a cusp behaviour for $r \gtrsim 0.03$ pc.

Linear evolution from random initial conditions

Profiles averaged in the angles for 500 random initial conditions. $\rho(r)/\rho(0)$ vs. $r/r_{1/4}$ [Destri, de Vega, Sanchez, in preparation]. Burkert and Pseudothermal profiles $\rho(r)/\rho(0)$ vs. $r/r_{1/4}$.

Linear CDM profiles are cusped
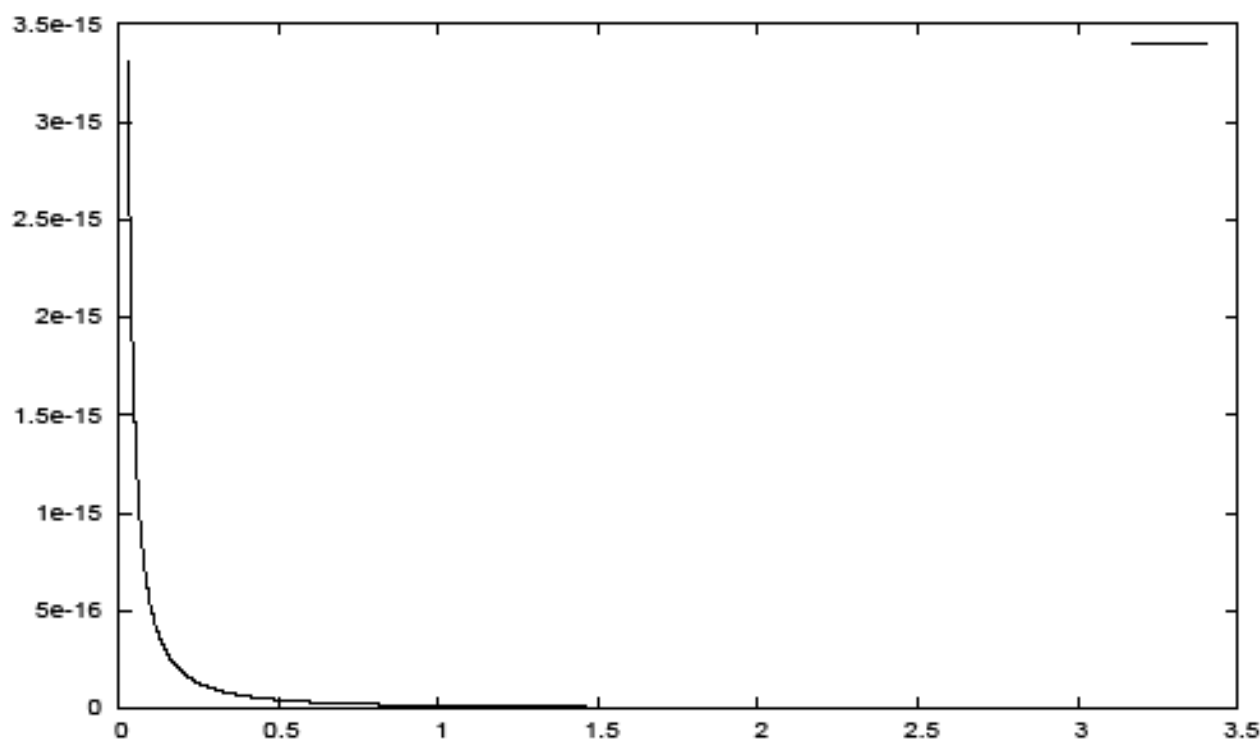
$\rho_{lin}(r)_{CDM}$ in g/cm^3 vs. r in pc.
Exhibits a cusp behaviour for $r \gtrsim 0.03$ pc. (Here $m_{CDM} = 100$ GeV).
Observations in DM dominated galaxies always exhibit cores.

WDM vs CDM linear fluctuations Today
Destri, de Vega Sanchez, in preparation
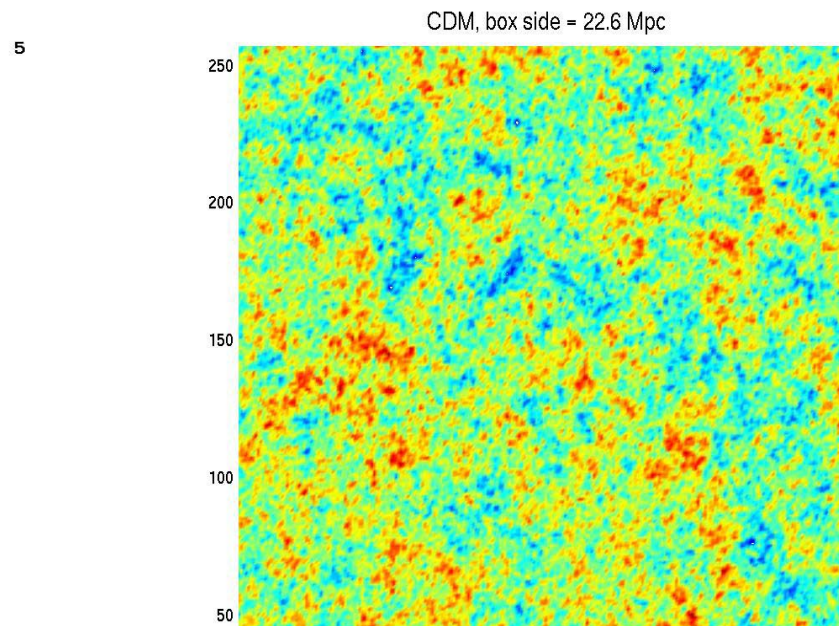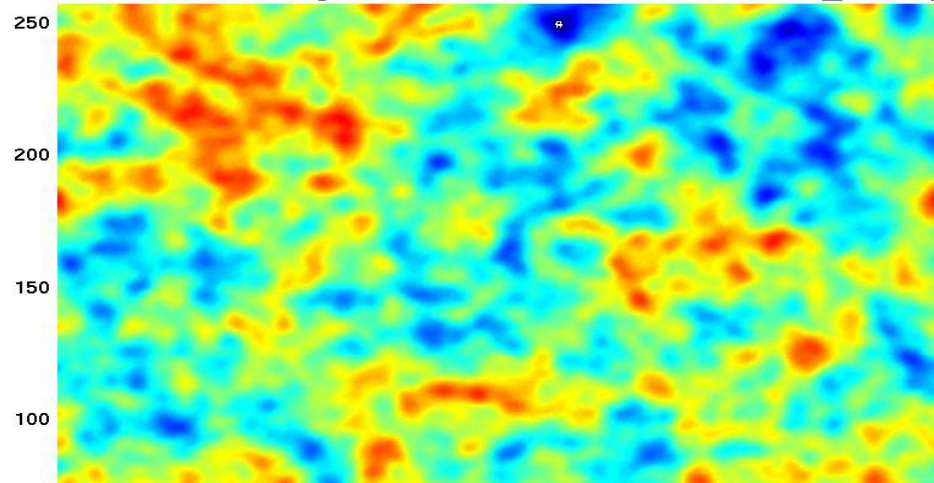
Box side = 22.6 Mpc

CDM, box side = 22.6 Mpc

keV SCALE DARK MATTER PARTICLES REPRODUCE:

→**OBSERVED GALAXY DENSITIES AND VELOCITY DISPERSIONS**

→**OBSERVED GALAXY DENSITY PROFILES**

→**OBSERVED SURFACE DENSITY VALUES OF DARK MATTER DOMINATED GALAXIES**

Particle physics candidates for DM

No particle in the Standard Model of particle physics (SM) can play the role of DM.

Many extensions of the SM can be envisaged to include a DM particle with mass in the keV scale and weakly enough coupled to the Standard Model particles to fulfill all particle physics experimental constraints.

Main candidates in the keV mass scale: sterile neutrinos, gravitinos, light neutralino, majoron ...

Particle physics motivations for sterile neutrinos:

There are both left and right handed quarks (with respect to the chirality).

It is natural to have right handed neutrinos ν_R besides the known left-handed neutrino. Quark-lepton similarity.

Summary: keV scale DM particles

- **Reproduce** the phase-space density observed in dwarf satellite galaxies and spiral galaxies (dV S 2009).

- Provide cored universal galaxy profiles in agreement with observations (dV S 2009,dV S S 2010). (Review on cores vs. cusps by de Blok 2010, Salucci & Frigerio Martins 2009)

- Reproduce the universal surface density μ_0 of DM dominated galaxies (dV S S 2010). WIMPS simulations give 1000 times the observed value of μ_0 (Hoffman et al. 2007).

- **Alleviate** the satellite problem which appears when wimps are used (Avila-Reese et al. 2000, Götz & Sommer-Larsen 2002)

- **Alleviate** the voids problem which appears when wimps are used (Tikhonov et al. 2009).

Summary: keV scale DM particles

- **All direct searches** of DM particles look for $m \gtrsim 1$ GeV. DM mass in the keV scale explains why nothing has been found ... e^+ and $\bar{p}$ excess in cosmic rays may be explained by astrophysics: P. L. Biermann et al. (2009), P. Blasi, P. D. Serpico (2009).

- Galaxies from Wimps simulations are too small (Ryan Joung et al. 2009, Holz & Perlmutter 2010). keV scale DM may alleviate this problem.

- Velocity widths in galaxies from 21cm HI surveys. ALFALFA survey clearly favours WDM over CDM. Papastergis et al. 2011, Zavala et al. 2009

Reliable simulations with keV mass DM are needed to clarify all these issues.

Summary and Conclusions

- Combining theoretical evolution of fluctuations through the Boltzmann-Vlasov equation with galaxy data points to a DM particle mass 3 - 10 keV. T_d may be $>$ or < 100 GeV. The keV mass scale holds independently of the DM particle physics model.

- Universal Surface density in DM galaxies $[\mu_{0D} \simeq (18 \text{ MeV})^3]$ explained by keV mass scale DM. Density profile scales and decreases for intermediate scales with the spectral index n_s: $\rho(r) \sim r^{-1-n_s/2}$ and $\rho(r) \sim r^{-2}$ for $r \gg r_0$.

H. J. de Vega, P. Salucci, N. G. Sanchez, 'The mass of the dark matter particle from theory and observations', arXiv:1004.1908.

H. J. de Vega, N. Sanchez, 'Model independent analysis of dark matter points to a particle mass at the keV scale', arXiv:0901.0922, MNRAS 404, 885 (2010).

[DARK MATTER : FACTS AND STATUS

→ DARK MATTER DOES EXIST

→ ASTROPHYSICAL OBSERVATIONS POINTS TO THE EXISTENCE OF DARK MATTER

→ AFTER MORE THAN TWENTY YEARS OF DEDICATED DARK MATTER PARTICLE EXPERIMENTS, THE DIRECT SEARCH OF DARK MATTER PARTICLES FULLY CONCENTRATED IN "GeV WIMPS" REVEALED SO FAR, UNSUCCEFULL. BUT DARK MATTER DOES EXIST

IN DESPITE OF THAT: PROPOSALS TO REPLACE DARK MATTER DID APPEARED:

PROPOSING TO CHANGE THE LAWS OF PHYSICS (!!!),   ADDING OVER CONFUSION, MIXING , POLLUTION...

TODAY, THE DARK MATTER RESEARCH AND DIRECT SEARCH SEEMS TO SPLIT IN THREE SETS:

(1). PARTICLE PHYSICS DARK MATTER: PARTICLE BUILDING MODELS, DEDICATED LAB EXPERIMENTS, ANNHILATING DARK MATTER, (FULLY CONCENTRATED ON "GeV WIMPS")

(2). ASTROPHYSICAL DARK MATTER: (ASTROPHYSICAL MODELS, ASTROPHYSICAL OBSERVATIONS)

(3). NUMERICAL SIMULATIONS

(1) and (2) DO NOT AGREE IN THE RESULTS
and (2) and (3) DO NOT FULLY AGREE NEITHER

SOMETHING IS GOING WRONG IN THE RESEARCH ON THE DARK MATTER

WHAT IS GOING WRONG ?, [AND WHY IS GOING WRONG]

THE SUBJECT IS MATURE

→ **THERE EXIST ASTRONOMICAL OBSERVATIONS AND FACILITIES**

→ **THERE EXIST MODEL /THEORETICAL ASTROPHYSICAL RESULTS WHICH FIT, AGREE WITH THE ASTRONOMICAL OBSERVATIONS**

→ **THERE EXISTED, THERE EXIST MANY DARK MATTER DEDICATED PARTICLE EXPERIMENTS (ALTHOUGH FULLY CONCENTRATED IN "GeV WIMPS")**

→ **THERE EXIST COMPUTER AND SUPER COMPUTERS AND DIFFERENT RESEARCHER GROUPS PERFORMING WORK WITH THEM**

→ **THERE EXIST A CONSIDERABLE AMOUNT OF RESEARCHERS WORKING IN DARK MATTER DURING MORE THAN TWENTY YEARS**

" FUITE EN AVANT" ("ESCAPE TO THE FUTURE") IS NOT THE ISSUE WHAT IS WRONG in the present day subject of Dark Matter?, (The Answer is Trivial and can be found in these 3 slides)   ]

DM Dark Matter research

- **Present CDM status:** Always increasing amount of confusion in the CDM research in the last 20 years , namely the increasing number and ciclic changing of arguments and counter-arguments and ad-hoc mechanisms introduced in CDM simulations over most of twenty years, in trying to deal with the CDM small scale problems, without really having a physical first principle derivation or control of such invoked mechanisms for the purpose ("adiabatic contraction", non circular motions, triaxiality, mergers, baryon feedbacks, strippings,,...", ...)
-

(C)DM research: present status

- **On the CDM particle side,** the problems are no less critical: So far, all the dedicated experimental searches after most of twenty years to find the theoretically proposed CDM particle candidats (Wimps) have failed.

- Its **indirect search** (invoking **"CDM annihilation"**) to explain cosmic rays positron excess, is in crisis as well, as wimps annihilation models are plugged with increasing tailoring or fine tuning, and such cosmic rays excesses are well explained and reproduced naturally by natural astrophysical process.

- The so-called and repeatedly invoked **"`wimp miracle"** is nothing but one equation with three constraints, theoretically motivated by SUSY model building.

Summary (3) (Pasquale BLASI, here on Wednesday)

THIS IS ESPECIALLY TO BE KEPT IN MIND WHEN INVOKING UNCONVENTIONAL EXPLANATIONS, SUCH AS THOSE BASED ON COLD DARK MATTER ANNIHILATION

THE DM HYPOTHESIS FOR THE POSITRON EXCESS WAS NOT THE MOST NATURAL - THE SIGNAL FROM WIMPS IS NATURALLY TOO SMALL

BUT THE THEORY WAS CONTRIVE (LEPTOPHILIC DM, BOOST FACTORS,

SOMMERFIELD ENHANCEMENT) FOR THE SOLE PURPOSE OF FITTING ONE SET OF DATA (THE POSITRON FRACTION AND THE ABSENCE OF ANTIPROTON ANOMALIES).

(C)DM research: present status

- **The community engaged in CDM simulations and the super- computers is large, as well as the experimental particle physics wimp community, involving big budgets, (and large number of people), it could not then a rapid turning point which could be expected yet in the CDM research community.....**

- **Still, the situation is changing rapidly in the scientific WDM research, (simply because the subject is new and WDM (essentially) works….**

- **Wimp experiments will not find the DM particle …..**
- **LHC will not find the DM particle …..**
- **Simply because they are searching at the wrong DM mass scale**
- **The DM particle is at the keV scale**

Future Perspectives

The Golden Age of Cosmology and Astrophysics continues.

Galaxy and Star formation. DM properties from galaxy observations. Better upper bounds on DM cross-sections.

DM in planets and the earth. Flyby and Pioneer anomalies?

Chandra, Suzaku X-ray data: keV mass DM decay?

Sun models well reproduce the sun's chemical composition but not the heliosismology (Asplund et al. 2009).
Can DM inside the Sun help to explain the discrepancy?

Nature of Dark Matter? 83% of the matter in the universe.

Light DM particles are strongly favoured $m_{DM} \sim$ keV.
Sterile neutrinos ? Other particle in the keV mass scale?

Precision determination of DM properties (mass, T_d, nature) from better galaxy data combined with theory (Boltzmann-Vlasov and simulations).

Recent Chalonge Conferences and Workshops

Highlights and Conclusions of the Chalonge 14th Paris Cosmology Colloquium 2010: 'The Standard Model of the Universe: Theory and Observations'. P Biermann, D Boyanovsky, A Cooray, C Destri, H de Vega, G Gilmore, S Gottlober, E Komatsu, S McGaugh, A Lasenby, R Rebolo, P Salucci, N Sanchez and A Tikhonov present their highlights of the Colloquium.
Conclusions by H. J. de Vega, M.C. Falvella, N. G. Sanchez, arXiv:1009.3494, 58 pages, 20 figures.

Highlights and Conclusions of the Chalonge Meudon Workshop Dark Matter in the Universe. P Biermann, A Cavaliere, H J. de Vega, G Gentile, C Jog, A Lapi, P Salucci, N G. Sanchez, P Serpico, R Stiele, J van Eymeren and M Weber present their highlights of the Workshop.
Conclusions by H. J. de Vega, N. G. Sanchez, arXiv:1007.2411, 41 pages, 10 figures.

Sterile Neutrinos in the SM of particle physics

SM symmetry group: $SU(3)_{color} \otimes SU(2)_{weak} \otimes U(1)_{hypercharge}^{weak}$

Leptons are color singlets and doublets under weak SU(2).

Sterile neutrinos ν_R do not participate to weak interactions. Hence, they must be singlets of color, weak SU(2) and weak hypercharge.

The SM Higgs Φ is a SU(2) doublet with a nonzero vacuum expectation value Φ_0. It can couple Yukawa-type with the left and right handed leptons:

$$L_{Yuk} = y \, \bar{\nu}_L \, \nu_R \, \Phi_0 + h.c. \quad ,$$

$y =$ Yukawa coupling, $\quad \Phi_0 = \begin{pmatrix} 0 \\ v \end{pmatrix} \quad , \quad v = 174$ GeV.

This induces a mixing (bilinear) term between ν_L and ν_R which produces transmutations of $\nu_L \Leftrightarrow \nu_R$.

Sterile Neutrinos in the SM of particle physics

SM symmetry group: $SU(3)_{color} \otimes SU(2)_{weak} \otimes U(1)_{hypercharge}$

Leptons are color singlets and doublets under weak SU(2).

Sterile neutrinos ν_R do not participate to weak interactions. Hence, they must be singlets of color, weak SU(2) and hypercharge.

Mixing (bilinear) terms appear: $\bar{\Phi}_0 \, \bar{\nu}_R \, \nu_L$ and $\bar{\nu}_L \, \nu_R \, \Phi_0$. They produce transmutations $\nu_L \Leftrightarrow \nu_R$. ($m_D = h_Y \, |\Phi_0|$).

Neutrino mass matrix: $(\bar{\nu}_L \ \bar{\nu}_R) \begin{pmatrix} 0 & m_D \\ m_D & M \end{pmatrix} \begin{pmatrix} \nu_L \\ \nu_R \end{pmatrix}$

Seesaw mass eigenvalues: $\frac{m_D^2}{M}$ and M, with eigenvectors:

- active neutrino: $\nu_{active} \simeq \nu_L - \frac{m_D}{M} \, \nu_R, \quad M \gg m_D.$

- sterile neutrino: $\nu_{sterile} \simeq \nu_R + \frac{m_D}{M} \, \nu_L, \quad M \gg m_D^2/M.$

Sterile Neutrinos

Choosing $M \sim 1$ keV and $m_D \sim 0.1$ eV is consistent with observations.

Mixing angle: $\theta \sim \frac{m_D}{M} \sim 10^{-4}$ is appropriate to produce enough sterile neutrinos accounting for the observed DM.

Smallness of θ makes the detection of steriles very difficult.

Precise measure of nucleus recoil in tritium beta decay: $^3H_1 \Longrightarrow \, ^3He_2 + e^- + \bar{\nu}$ can show the presence of a sterile instead of the active $\bar{\nu}$ in the decay products.

Rhenium 187 beta decay gives $\theta < 0.095$ for 1 keV steriles [Galeazzi et al. PRL, 86, 1978 (2001)].
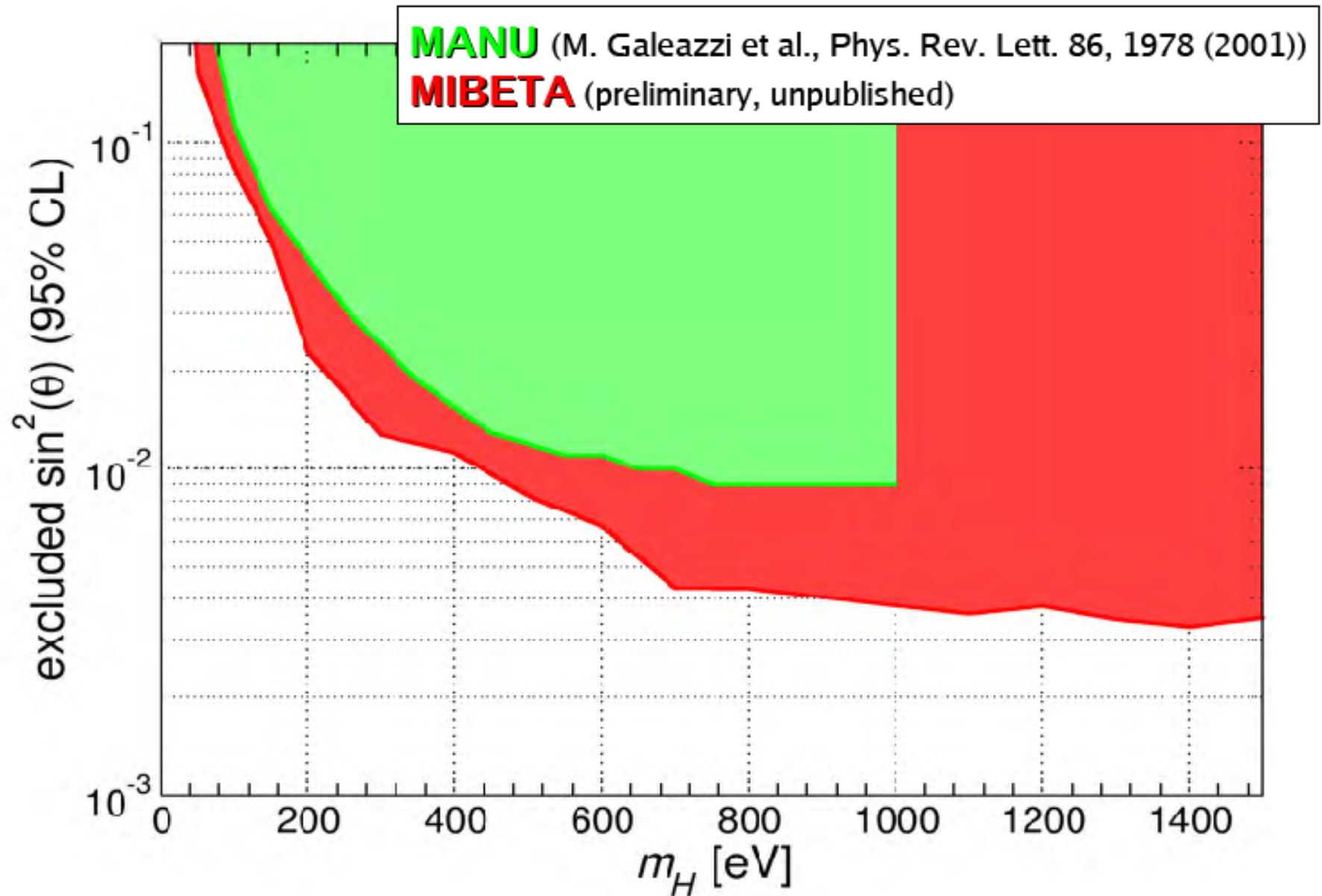Available energy: $Q(^{187}Re) = 2.47$ keV, $Q(^3H_1) = 18.6$ keV.

Conclusion: the empty slot of right-handed neutrinos in the Standard Model of particle physics can be filled by keV-scale sterile neutrinos describing the DM.
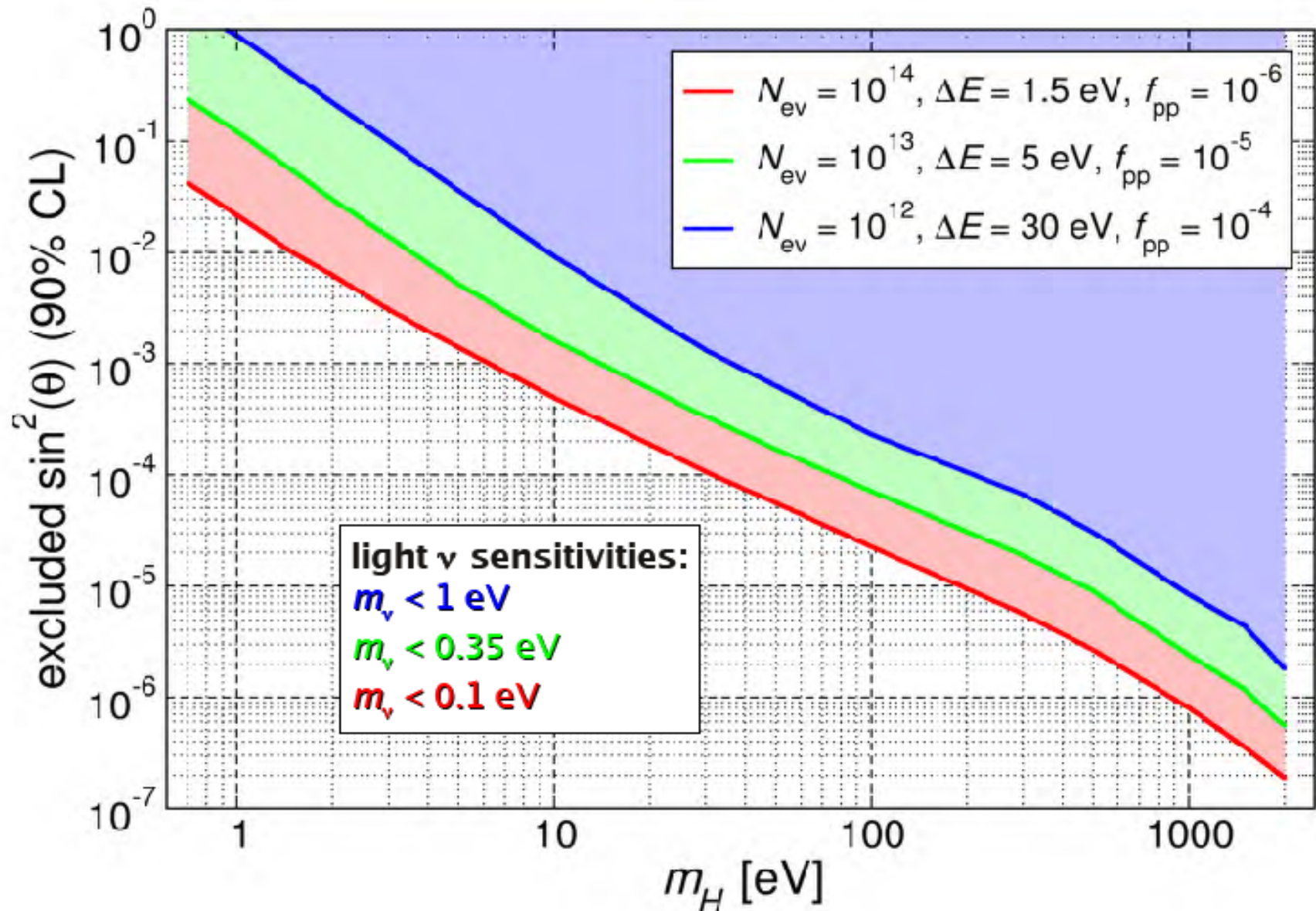
Sterile neutrino models

Sterile neutrinos: name coined by Bruno Pontecorvo (1968).

- DW: Dodelson-Widrow model (1994) sterile neutrinos produced by non-resonant mixing from active neutrinos.

- Shi-Fuller model (1998) sterile neutrinos produced by resonant mixing from active neutrinos.

- χ-model (1981)-(2006) sterile neutrinos produced by a Yukawa coupling from a real scalar χ.

- Further models can be proposed...

MANU (M. Galeazzi et al., Phys. Rev. Lett. 86, 1978 (2001))
MIBETA (preliminary, unpublished)

MARE sensitivity to heavy neutrinos: ^{187}Re option

The chart shows excluded $\sin^2(\theta)$ (90% CL) versus m_H [eV].

Legend:
- $N_{ev} = 10^{14}$, $\Delta E = 1.5$ eV, $f_{pp} = 10^{-6}$
- $N_{ev} = 10^{13}$, $\Delta E = 5$ eV, $f_{pp} = 10^{-5}$
- $N_{ev} = 10^{12}$, $\Delta E = 30$ eV, $f_{pp} = 10^{-4}$

light ν sensitivities:
$m_\nu < 1$ eV
$m_\nu < 0.35$ eV
$m_\nu < 0.1$ eV

END

THANK YOU

FOR YOUR ATTENTION